

**Supporting information for**

**Iron carbonyl cluster-incorporated Cu(I) NHC complexes in homocoupling  
of arylboronic acids: an effective  $[TeFe_3(CO)_9]^{2-}$  ligand**

Chien-Nan Lin,<sup>a</sup> Chung-Yi Huang,<sup>a</sup> Chia-Chi Yu,<sup>a</sup> Yen-Ming Chen,<sup>a</sup> Wei-Ming Ke,<sup>a</sup>  
Guan-Jung Wang,<sup>a</sup> Gon-Ann Lee<sup>\*b</sup> and Minghuey Shieh<sup>\*a</sup>

Department of Chemistry, National Taiwan Normal University, Taipei 11677, Taiwan,  
Republic of China

Department of Chemistry, Fu Jen Catholic University, Xinzhuang, New Taipei 24205, Taiwan,  
Republic of China

## Contents

<b>Experimental Section</b>	S2-S8
<b>Optimization of <math>[\text{TeFe}_3(\text{CO})_9\text{Cu}_2(\text{MeCN})_2]</math>- and <b>1–4</b>-Catalyzed Homocoupling of 4-Bromophenylboronic Acid</b>	S9-S10
<b>Electrochemical Measurements</b>	S10-S11
<b>X-ray Structural Characterization of <b>1–4</b></b>	S11-S12
<b>Explanations for the Checkcif Alert</b>	S13
<b>Computational Details</b>	S14
<b>References</b>	S15-S18
<b>Table S1.</b> $[\text{TeFe}_3(\text{CO})_9\text{Cu}_2(\text{MeCN})_2]$ - and <b>1–4</b> -catalyzed homocoupling of 4-bromophenylboronic acid: the optimization of the reaction conditions	S19
<b>Table S2.</b> The reported catalytic systems for homocoupling of 4-bromophenylboronic acid	S20
<b>Table S3.</b> Results of natural bond order of $[\text{TeFe}_3(\text{CO})_9\text{Cu}_2(\text{MeCN})_2]$ and <b>1–4</b>	S21
<b>Table S4.</b> Differential pulse voltammetry of $[\text{TeFe}_3(\text{CO})_9\text{Cu}_2(\text{MeCN})_2]$ and <b>1–4</b>	S22
<b>Table S5.</b> Crystallographic data for <b>1–4</b>	S23
<b>Table S6.</b> Selected bond distances and bond angles for <b>1–4</b>	S24-S26
<b>Table S7.</b> Electronic energy and cartesian coordinates of <b>1</b>	S27-S28
<b>Table S8.</b> Electronic energy and cartesian coordinates of <b>2</b>	S29-S30
<b>Table S9.</b> Electronic energy and cartesian coordinates of <b>3</b>	S31-S32
<b>Table S10.</b> Electronic energy and cartesian coordinates of <b>4</b>	S33-S34
<b>Figure S1.</b> PXRD patterns for crystals of <b>1</b> exposure to air for 10 days	S35
<b>Figure S2.</b> ORTEP diagram of <b>2</b>	S36
<b>Figure S3.</b> ORTEP diagram of <b>3</b>	S37
<b>Figure S4.</b> ORTEP diagram of <b>4</b>	S38
<b>Figure S5.</b> The proposed mechanism for the homocoupling of 4-bromophenylboronic acid	S39
<b>Figure S6.</b> Spatial graphs of frontier molecular orbitals for $[\text{TeFe}_3(\text{CO})_9\text{Cu}_2(\text{MeCN})_2]$ and <b>1–4</b>	S40
<b>Figure S7.</b> Correlation of product ratios with the Hammett equation	S41
<b>Spectroscopic Data of Products</b>	S42-S50

## Experimental Section

All reactions were performed under an atmosphere of pure nitrogen using standard Schlenk techniques.<sup>1</sup> Solvents were purified, dried, and distilled under nitrogen prior to use. KO*t*Bu, 3-nitrophenylboronic acid, 4-methoxyphenylboronic acid (all ACROS), 2-bromophenylboronic acid (AK Scientific), 3-bromophenylboronic acid (AK Scientific), 4-bromophenylboronic acid (Lancaster), and 4-nitrophenylboronic acid (Lancaster) were used as received. [Et<sub>4</sub>N]<sub>2</sub>[TeFe<sub>3</sub>(CO)<sub>9</sub>],<sup>2</sup> [Cu(MeCN)<sub>4</sub>][BF<sub>4</sub>],<sup>3</sup> [TeFe<sub>3</sub>(CO)<sub>9</sub>Cu<sub>2</sub>(MeCN)<sub>2</sub>],<sup>4</sup> [Cu<sub>2</sub>(MeIm(CH<sub>2</sub>)<sub>2</sub>ImMe)<sub>2</sub>][PF<sub>6</sub>]<sub>2</sub>,<sup>5</sup> and the imidazolium salts, 1,3-dimethylimidazolium iodide (Me<sub>2</sub>Im·HI),<sup>6a</sup> 1,1'-dimethyl-3,3'-methylene-diimidazolium diiodide (MeImCH<sub>2</sub>ImMe·H<sub>2</sub>I<sub>2</sub>),<sup>6b</sup> 1,1'-dimethyl-3,3'-ethylene-diimidazolium dibromide (MeIm(CH<sub>2</sub>)<sub>2</sub>ImMe·H<sub>2</sub>Br<sub>2</sub>),<sup>6a</sup> and 1,1'-dimethyl-3,3'-propylene-diimidazolium diiodide (MeIm(CH<sub>2</sub>)<sub>3</sub>ImMe·H<sub>2</sub>I<sub>2</sub>)<sup>6c</sup> were prepared according to the published methods. Chromatographic purification of compounds was achieved with Merck 60 silica gel (40–63 μm). Analytical thin layer chromatography (TLC) was performed on Silica Gel 60 F254 precoated plates. Infrared spectra were recorded on a Perkin-Elmer Paragon 1000 IR spectrometer. The NMR spectra were obtained on a Bruker AV 400 at 400.13 MHz for <sup>1</sup>H and 100.61 MHz for <sup>13</sup>C or on a Bruker AV 500 at 500.13 MHz for <sup>1</sup>H and 125.76 MHz for <sup>13</sup>C. <sup>1</sup>H and <sup>13</sup>C chemical shifts are reported in parts per million and were calibrated relative to DMSO-*d*<sub>6</sub> (<sup>1</sup>H: 2.49 ppm, <sup>13</sup>C: 39.51 ppm) as the internal standard. Elemental analyses for

C, H, and N were performed on a Perkin-Elmer 2400 analyzer at the MOST Regional Instrumental Center at National Taiwan University, Taipei, Taiwan.

**Synthesis of  $[\text{TeFe}_3(\text{CO})_9\text{Cu}_2(\text{Me}_2\text{Im})_2]$  (1).** A THF solution (20 mL) of  $[\text{TeFe}_3(\text{CO})_9\text{Cu}_2(\text{MeCN})_2]$  (0.30 g, 0.40 mmol),  $\text{Me}_2\text{Im} \cdot \text{HI}$  (0.18 g, 0.80 mmol), and  $\text{KO}^t\text{Bu}$  (0.090 g, 0.80 mmol) was stirred at ambient temperature overnight. The resultant solution was filtered, and the solvent was evaporated under vacuum. The residue was washed with deionized water and hexanes several times and then extracted with  $\text{CH}_2\text{Cl}_2$  to give a purplish-brown solution, which was recrystallized with hexanes/MeOH/ $\text{CH}_2\text{Cl}_2$  to give  $[\text{TeFe}_3(\text{CO})_9\text{Cu}_2(\text{Me}_2\text{Im})_2]$  (1) (yield 0.19 g, 0.22 mmol, 55 % based on  $[\text{TeFe}_3(\text{CO})_9\text{Cu}_2(\text{MeCN})_2]$ ). IR ( $\nu_{\text{CO}}$ ,  $\text{CH}_2\text{Cl}_2$ ): 2031 (m), 1972 (vs), 1918 (w)  $\text{cm}^{-1}$ .  $^1\text{H}$  NMR (500 MHz, DMSO- $d_6$ , 300 K, ppm):  $\delta$  7.30 (s, 4H, NCH), 3.77 (s, 12H,  $\text{NCH}_3$ ).  $^{13}\text{C}$  NMR (125 MHz, DMSO- $d_6$ , 300 K, ppm):  $\delta$  218.90 (Fe-CO), 178.20 ( $C_{\text{carbene}}$ ), 122.00 (NCH), 37.18 ( $\text{NCH}_3$ ). Anal. Calcd for  $\text{C}_{19}\text{H}_{16}\text{Cu}_2\text{Fe}_3\text{N}_4\text{O}_9\text{Te}$ : C, 26.33; H, 1.86; N, 6.47. Found: C, 26.10; H, 2.12; N, 6.48. Mp: 166 °C dec. Crystals of  $[\text{TeFe}_3(\text{CO})_9\text{Cu}_2(\text{Me}_2\text{Im})_2]$  (1) suitable for X-ray diffraction were grown from hexanes/MeOH/ $\text{CH}_2\text{Cl}_2$ .

**Synthesis of  $[\text{TeFe}_3(\text{CO})_9\text{Cu}_2(\text{MeImCH}_2\text{ImMe})]$  (2). Method 1.** A THF solution (20 mL) of  $[\text{TeFe}_3(\text{CO})_9\text{Cu}_2(\text{MeCN})_2]$  (0.60 g, 0.79 mmol),  $\text{MeImCH}_2\text{ImMe} \cdot \text{H}_2\text{I}_2$  (0.34 g, 0.79 mmol), and  $\text{KO}^t\text{Bu}$  (0.18 g, 1.60 mmol) was stirred at 40 °C overnight. The reddish-brown solution was filtered, and the solvent was evaporated under vacuum. The

residue was extracted with Et<sub>2</sub>O to give a purplish-brown solution and evaporated under vacuum again. The solid was washed with deionized water and hexanes several times and then extracted with CH<sub>2</sub>Cl<sub>2</sub> to give a purplish-brown solution, which was recrystallized with hexanes/MeOH/CH<sub>2</sub>Cl<sub>2</sub> to give [TeFe<sub>3</sub>(CO)<sub>9</sub>Cu<sub>2</sub>(MeImCH<sub>2</sub>ImMe)] (**2**) (yield 0.14 g, 0.16 mmol, 20% based on [TeFe<sub>3</sub>(CO)<sub>9</sub>Cu<sub>2</sub>(MeCN)<sub>2</sub>]). IR ( $\nu_{\text{CO}}$ , CH<sub>2</sub>Cl<sub>2</sub>): 2033 (m), 2023 (w), 1987 (vs), 1974 (s), 1934 (w), 1892 (m) cm<sup>-1</sup>. <sup>1</sup>H NMR (400 MHz, DMSO-*d*<sub>6</sub>, 300 K, ppm):  $\delta$  7.70 (s, 2H, NCH), 7.39 (s, 2H, NCH), 6.54 (br, 1H, NCH<sub>2</sub>N), 6.40 (br, 1H, NCH<sub>2</sub>N), 3.77 (s, 6H, NCH<sub>3</sub>). <sup>13</sup>C NMR (100 MHz, DMSO-*d*<sub>6</sub>, 300 K, ppm):  $\delta$  218.27 (Fe-CO), 177.18 (C<sub>carbene</sub>), 123.40, 120.99 (NCH), 62.10 (NCH<sub>2</sub>N), 37.63 (NCH<sub>3</sub>). Anal. Calcd for C<sub>18</sub>H<sub>12</sub>Cu<sub>2</sub>Fe<sub>3</sub>N<sub>4</sub>O<sub>9</sub>Te: C, 25.42; H, 1.42; N, 6.59. Found: C, 25.53; H, 1.65; N, 6.67. Mp: 166 °C dec. Crystals of [TeFe<sub>3</sub>(CO)<sub>9</sub>Cu<sub>2</sub>(MeImCH<sub>2</sub>ImMe)] (**2**) suitable for X-ray diffraction were grown from hexanes/MeOH/CH<sub>2</sub>Cl<sub>2</sub>.

*Method 2.* Freshly dried THF (10 mL) was added to a mixture of MeImCH<sub>2</sub>ImMe·H<sub>2</sub>I<sub>2</sub> (0.173 g, 0.40 mmol) and KO<sup>t</sup>Bu (0.090 g, 0.80 mmol), and the mixture was stirred in an ice-water bath for 2 h. The resultant solution was filtered, and the pale yellow filtrate was then transferred to a THF solution (10 mL) of [TeFe<sub>3</sub>(CO)<sub>9</sub>Cu<sub>2</sub>(MeCN)<sub>2</sub>] (0.30 g, 0.40 mmol), which was stirred for another 30 min. The resultant solution was filtered, and the solvent was removed under vacuum. The residue was washed with deionized water and hexanes several times and then extracted with CH<sub>2</sub>Cl<sub>2</sub> to give a purplish-brown solution, which was

recrystallized with hexanes/MeOH/CH<sub>2</sub>Cl<sub>2</sub> to give [TeFe<sub>3</sub>(CO)<sub>9</sub>Cu<sub>2</sub>(MeImCH<sub>2</sub>ImMe)] (**2**) (yield 0.14 g, 0.16 mmol, 40% based on [TeFe<sub>3</sub>(CO)<sub>9</sub>Cu<sub>2</sub>(MeCN)<sub>2</sub>]).

**Synthesis of [TeFe<sub>3</sub>(CO)<sub>9</sub>Cu<sub>2</sub>(MeIm(CH<sub>2</sub>)<sub>2</sub>ImMe)] (**3**).** *Method 1.* A THF solution (20 mL) of [TeFe<sub>3</sub>(CO)<sub>9</sub>Cu<sub>2</sub>(MeCN)<sub>2</sub>] (0.33 g, 0.44 mmol), MeIm(CH<sub>2</sub>)<sub>2</sub>ImMe·H<sub>2</sub>Br<sub>2</sub> (0.16 g, 0.45 mmol), and KO'Bu (0.099 g, 0.88 mmol) was stirred at ambient temperature for 5 h. The resultant solution was filtered, and the solvent was evaporated under vacuum. The residue was extracted with Et<sub>2</sub>O to give a purplish-brown solution and evaporated under vacuum again. The solid was washed with deionized water and hexanes several times and then extracted with CH<sub>2</sub>Cl<sub>2</sub> to give a purplish-brown solution, which was recrystallized with hexanes/MeOH/CH<sub>2</sub>Cl<sub>2</sub> to give [TeFe<sub>3</sub>(CO)<sub>9</sub>Cu<sub>2</sub>(MeIm(CH<sub>2</sub>)<sub>2</sub>ImMe)] (**3**) (yield 0.079 g, 0.091 mmol, 21 % based on [TeFe<sub>3</sub>(CO)<sub>9</sub>Cu<sub>2</sub>(MeCN)<sub>2</sub>]). IR ( $\nu_{\text{CO}}$ , CH<sub>2</sub>Cl<sub>2</sub>): 2032 (m), 1985 (vs), 1967 (m), 1955 (m) cm<sup>-1</sup>. <sup>1</sup>H NMR (400 MHz, DMSO-*d*<sub>6</sub>, 300 K, ppm):  $\delta$  7.31 (s, 2H, NCH), 7.22 (s, 2H, NCH), 4.58 (s, 4H, NCH<sub>2</sub>CH<sub>2</sub>N), 3.74 (s, 6H, NCH<sub>3</sub>). <sup>13</sup>C NMR (100 MHz, DMSO-*d*<sub>6</sub>, 298 K, ppm):  $\delta$  218.44 (Fe-CO), 176.60 (C<sub>carbene</sub>), 122.34, 121.32 (NCH), 50.58 (NCH<sub>2</sub>CH<sub>2</sub>N), 37.48 (NCH<sub>3</sub>). Anal. Calcd for C<sub>19</sub>H<sub>14</sub>Cu<sub>2</sub>Fe<sub>3</sub>N<sub>4</sub>O<sub>9</sub>Te: C, 26.40; H, 1.63; N, 6.48. Found: C, 26.62; H, 1.79; N, 6.81. Mp: 171 °C dec. Crystals of [TeFe<sub>3</sub>(CO)<sub>9</sub>Cu<sub>2</sub>(MeIm(CH<sub>2</sub>)<sub>2</sub>ImMe)] (**3**) suitable for X-ray diffraction were grown from hexanes/MeOH/CH<sub>2</sub>Cl<sub>2</sub>.

*Method 2.* Freshly dried THF (15 mL) was added to a mixture of MeIm(CH<sub>2</sub>)<sub>2</sub>ImMe·H<sub>2</sub>Br<sub>2</sub>

(0.19 g, 0.54 mmol) and KO'Bu (0.12 g, 1.07 mmol), and the mixture was stirred in an ice-water bath for 3 h. The resultant solution was filtered, and the pale yellow filtrate was then transferred to a THF solution (10 mL) of  $[\text{TeFe}_3(\text{CO})_9\text{Cu}_2(\text{MeCN})_2]$  (0.40 g, 0.53 mmol), which was stirred for another 1.5 h. The resultant solution was filtered, and the solvent was removed under vacuum. The residue was extracted with  $\text{CH}_2\text{Cl}_2$  to give a purplish-brown solution and evaporated under vacuum again. The solid was washed with deionized water and hexanes several times and then extracted with THF to give a purplish-brown solution, which was recrystallized with hexanes/MeOH/THF to give  $[\text{TeFe}_3(\text{CO})_9\text{Cu}_2(\text{MeIm}(\text{CH}_2)_2\text{ImMe})]$  (**3**) (yield 0.23 g, 0.27 mmol, 51% based on  $[\text{TeFe}_3(\text{CO})_9\text{Cu}_2(\text{MeCN})_2]$ ).

**Synthesis of  $[\text{TeFe}_3(\text{CO})_9\text{Cu}_2(\text{MeIm}(\text{CH}_2)_3\text{ImMe})]$  (**4**). Method 1.** A THF solution (20 mL) of  $[\text{TeFe}_3(\text{CO})_9\text{Cu}_2(\text{MeCN})_2]$  (0.35 g, 0.46 mmol), MeIm( $\text{CH}_2$ )<sub>3</sub>ImMe·H<sub>2</sub>I<sub>2</sub> (0.21 g, 0.46 mmol), and KO'Bu (0.103 g, 0.92 mmol) was stirred at ambient temperature for 9 h. The resultant solution was filtered, and the solvent was evaporated under vacuum. The residue was washed with deionized water and hexanes several times and then extracted with  $\text{CH}_2\text{Cl}_2$  to give a purplish-brown solution, which was recrystallized with hexanes/MeOH/ $\text{CH}_2\text{Cl}_2$  to give  $[\text{TeFe}_3(\text{CO})_9\text{Cu}_2(\text{MeIm}(\text{CH}_2)_3\text{ImMe})]$  (**4**) (yield 0.043 g, 0.049 mmol, 11 % based on  $[\text{TeFe}_3(\text{CO})_9\text{Cu}_2(\text{MeCN})_2]$ ). IR ( $\nu_{\text{CO}}$ ,  $\text{CH}_2\text{Cl}_2$ ): 2032 (m), 1984 (vs), 1968 (m), 1956 (m)  $\text{cm}^{-1}$ . <sup>1</sup>H NMR (500 MHz, DMSO-*d*<sub>6</sub>, 300 K, ppm):  $\delta$  7.60 (br, 2H, NCH), 7.50 (br, 2H, NCH), 4.06 (s, 4H,  $\text{NCH}_2\text{CH}_2\text{CH}_2\text{N}$ ), 3.41 (br, 6H,  $\text{NCH}_3$ ), 2.43 (s, 2H,  $\text{NCH}_2\text{CH}_2\text{CH}_2\text{N}$ ). <sup>13</sup>C NMR

(125 MHz, DMSO-*d*<sub>6</sub>, 300 K, ppm):  $\delta$  218.94 (Fe-CO), 175.58 (*C*<sub>carbene</sub>), 123.75, 120.71 (NCH), 46.13 (NCH<sub>2</sub>CH<sub>2</sub>CH<sub>2</sub>N), 36.63 (NCH<sub>3</sub>), 29.65 (NCH<sub>2</sub>CH<sub>2</sub>CH<sub>2</sub>N). Anal. Calcd for C<sub>20</sub>H<sub>16</sub>Cu<sub>2</sub>Fe<sub>3</sub>N<sub>4</sub>O<sub>9</sub>Te: C, 27.34; H, 1.84; N, 6.38. Found: C, 27.68; H, 1.91; N, 6.38. Mp: 166 °C dec. Crystals of [TeFe<sub>3</sub>(CO)<sub>9</sub>Cu<sub>2</sub>(MeIm(CH<sub>2</sub>)<sub>3</sub>ImMe)] (**4**) suitable for X-ray diffraction were grown from hexanes/MeOH/CH<sub>2</sub>Cl<sub>2</sub>.

*Method 2.* Freshly dried THF (10 mL) was added to a mixture of MeIm(CH<sub>2</sub>)<sub>3</sub>ImMe·H<sub>2</sub>I<sub>2</sub> (0.184 g, 0.40 mmol) and KO'Bu (0.090 g, 0.80 mmol), and the mixture was stirred in an ice-water bath for 2 h. The resultant solution was filtered, and the pale yellow filtrate was then transferred to a THF solution (10 mL) of [TeFe<sub>3</sub>(CO)<sub>9</sub>Cu<sub>2</sub>(MeCN)<sub>2</sub>] (0.30 g, 0.40 mmol), which was stirred for another 30 min. The resultant solution was filtered, and the solvent was removed under vacuum. The residue was washed with deionized water and hexanes several times and then extracted with CH<sub>2</sub>Cl<sub>2</sub> to give a purplish-brown solution, which was recrystallized with hexanes/MeOH/CH<sub>2</sub>Cl<sub>2</sub> to give [TeFe<sub>3</sub>(CO)<sub>9</sub>Cu<sub>2</sub>(MeIm(CH<sub>2</sub>)<sub>3</sub>ImMe)] (**4**) (yield 0.17 g, 0.19 mmol, 48% based on [TeFe<sub>3</sub>(CO)<sub>9</sub>Cu<sub>2</sub>(MeCN)<sub>2</sub>]).

### The General Procedure for the Homocoupling of 2-, 3-, or 4-Bromophenylboronic

**Acids Leading to Biaryls.** A solution of catalyst **1** (0.0050 mmol) and 2-, 3-, or 4-bromophenylboronic acids (1.00 mmol) in MeOH (3 mL) was stirred at 25 °C. The resultant reaction mixture was evaporated under vacuum. The residue was purified by flash chromatography on silica gel eluted with *n*-hexane to afford biaryls. To compare the

productivities of the catalysts, all the homocoupling reactions mentioned herein were carried out repeatedly and carefully to ensure accuracy.

### **The General Procedure for the Homocoupling of 3-Nitro- or**

**4-Methoxyphenylboronic Acids Leading to Biaryls.** A solution of catalyst **1** (0.0050 mmol) and 3-nitro- or 4-methoxyphenylboronic acids (1.00 mmol) in MeOH (3 mL) was stirred at 25 °C. The resultant reaction mixture was evaporated under vacuum. The residue was purified by flash chromatography on a silica gel column (petroleum ether/ethyl acetate, 5: 1) to afford biaryls. To compare the productivities of the catalysts, all the homocoupling reactions mentioned herein were carried out repeatedly and carefully to ensure accuracy.

### **The General Procedure for the Homocoupling of 4-Nitrophenylboronic Acids**

**Leading to Biaryls.** A solution of catalyst **1** (0.0050 mmol) and 4-nitrophenylboronic acid (1.00 mmol) in MeOH (3 mL) was stirred at 25 °C. The resultant reaction mixture was evaporated under vacuum. The residue was purified by flash chromatography on a silica gel column (petroleum ether/ethyl acetate, 5: 1) to afford 4,4'-dinitrobiphenyl (0.39 mmol, 78 %) and 4-nitrophenol (0.21 mmol, 21 %). To compare the productivities of the catalysts, the homocoupling reaction mentioned herein was carried out repeatedly and carefully to ensure accuracy.

## **Optimization of $[\text{TeFe}_3(\text{CO})_9\text{Cu}_2(\text{MeCN})_2]$ - and **1–4**-Catalyzed Homocoupling of**

**4-Bromophenylboronic Acid under Different Reaction Conditions.** In order to explore the behavior of  $[\text{TeFe}_3(\text{CO})_9\text{Cu}_2(\text{MeCN})_2]$  and **1–4** in catalyzing Suzuki homocoupling reactions, complex **1** was chosen as the model catalyst and 4-bromophenylboronic acid was chosen as the model substrate to optimize catalytic conditions (Table S1). We found that complex **1** (2.0 mol% of Cu loading) exhibited good catalytic performances in the homocoupling of 4-bromophenylboronic acid in MeOH at room temperature in air, without any additives such as a base or a ligand, affording the 4,4'-dibromobiphenyl product in an 84% yield (Table S1, Entry 1), which indicated that a catalytic cycle was operating under the current conditions. In the absence of catalyst **1** or under  $\text{N}_2$ , this homocoupling reaction did not occur (Entries 2-4). Moreover, when 3 mol% of Fe loading of catalyst  $[\text{Et}_4\text{N}]_2[\text{TeFe}_3(\text{CO})_9]$  was used, no biaryl products were observed, indicating that Cu was essential for the catalytic performance (Entry 5). We next examined the effect of the polar protic or aprotic solvents (Entries 6-9); however, the protic methanol was still the best choice (Entry 1). The reaction temperature had great influence on this reaction. When the temperature was increased to the refluxing MeOH temperature, the product was formed in a lower yield (27%) (Entry 10), indicating the thermal instability of catalyst **1**. Notably, when  $\text{O}_2$  was introduced into the system, the time required for the completion of the reaction reduced to 1 h and the yield maintained at a good yield (85 %) (Entry 11), suggesting that sufficient  $\text{O}_2$  was necessary. On the other hand, the

influence of the amount of complex **1** on the reaction was also examined. The results showed that a Cu loading (1.0 mol%) of catalyst **1** gave the best reaction condition with 88% yield (Entry 12), however, the lower Cu loading (0.5 mol%) required the longer reaction time (12 h) for completion of the reaction (Entry 13). Other catalysts like **2–4** and  $[\text{TeFe}_3(\text{CO})_9\text{Cu}_2(\text{MeCN})_2]$  were also used to catalyze the homocoupling of 4-bromophenylboronic acid under conditions that included 1.0 mol% of Cu loading, methanol as the solvent, room temperature, an atmosphere of  $\text{O}_2$ , and without any additives such as bases, ligands, or other oxidants (Entries 14–17).

**Electrochemical Measurements.** The electrochemical measurements were performed at room temperature under a nitrogen atmosphere and recorded using a CHI 621D electrochemical potentiostat. A glassy carbon working electrode, a platinum wire auxiliary electrode, and a non-aqueous  $\text{Ag}/\text{Ag}^+$  electrode were used in a three-electrode configuration. Tetra-*n*-butylammonium perchlorate (TBAP) was used as the supporting electrolyte, and the solute concentration was  $\sim 10^{-3}$  M. The redox potentials were calibrated with a ferrocenium/ferrocene ( $\text{Fc}^+/\text{Fc}$ ) couple in the working solution and were referenced to SCE.

To explore the effect of the incorporation of the mono- or bidentate NHC ligands into the  $\text{TeFe}_3(\text{CO})_9\text{Cu}_2$  cluster core, the electrochemical behaviors of  $[\text{TeFe}_3(\text{CO})_9\text{Cu}_2(\text{MeCN})_2]$  and **1–4** were investigated by differential pulse voltammetry (DPV). For comparison, the DPVs of  $[\text{Cu}_2(\text{MeIm}(\text{CH}_2)_2\text{ImMe})_2][\text{PF}_6]_2$  and  $[\text{Cu}(\text{MeCN})_4]\text{[BF}_4]$  were performed as well.

Because of the irreversible desorption of Cu ( $-0.198$  to  $-0.489$  V),<sup>7</sup> the DPV profiles were only discussed between  $1.004$  and  $-0.20$  V. The DPV data are summarized in Table S4.

For the DPV analysis, the measurement of the peak width at the half height ( $W_{1/2}$ ) determined the electron stoichiometry.<sup>8a</sup>  $[\text{TeFe}_3(\text{CO})_9\text{Cu}_2(\text{MeCN})_2]$  and **1–4** exhibited similar redox behaviors and each showed two one-electron quasi-reversible oxidations ( $0.015 \sim 0.134$  V and  $0.232 \sim 0.286$  V) and a one-electron quasi-reversible reduction ( $-0.085 \sim -0.143$  V) (Table S4). The widths of the DPV peaks at the half-height ( $W_{1/2}$ ) of these complexes were a bit greater or lower than the value ( $W_{1/2} = 90$  mV) expected for the one-electron reversible redox couples, indicating that these DPV responses were quasi-reversible.<sup>8</sup>

**X-ray Structural Characterization of **1–4**.** Selected crystallographical data for **1–4** are given in Table S5. All crystals were mounted on glass fibers with epoxy cement. Data collections for **1**, **2**, and **4** were carried out on a Bruker Apex II CCD diffractometer with graphite-monochromated Mo K $\alpha$  radiation at  $200(2)$  K in the  $2\theta$  range of  $2.0\text{--}50.0^\circ$ . Data collection for **3** were carried out on a Bruker-Nonius Kappa CCD diffractometer with graphite-monochromated Mo K $\alpha$  radiation at  $200(2)$  K employing the  $\theta\text{--}2\theta$  scan mode. An empirical absorption correction by the multi-scan method was applied to the data using SADABS.<sup>9</sup> The structures of **1–4** were solved by direct methods and refined with SHELXL-97.<sup>10</sup> Each of **3** and **4** contained two independent but chemically similar asymmetric structures in the unit cell where their bond distances and angles were similar and

only one structure was described for further comparison. For complex **4**, in order to obtain reasonable thermal parameters, the N7 and C36 atoms were restrained by using SIMU and DELU commands and the C34 and C35 atoms were restrained by using DELU command during the least-squares refinement. The non-hydrogen atoms for all structures were refined with anisotropic temperature factors. The selected distances and angles for **1–4** are listed in Table S6. These Cu—C distances are within the van der Waals interaction (2.245(5)–2.863(6) Å, **1**; 2.268(5)–2.803(5) Å, **2**; 2.307(6)–2.597(6) Å, **3**; 2.296(4)–2.787(5) Å, **4**), and the corresponding Fe—C—O angles are slightly bent from 180° (166.3(5)–174.2(6)°, **1**; 160.2(5)–179.3(4)°, **2**; 167.3(5)–174.8(6)°, **3**; 166.0(4)–173.3(4)°, **4**) (Fig. 1 and S2–S4).

### **Explanation for the Checkcif Alert for 4:**

 **Alert level B**  
PLAT029 ALERT 3 B] \_diffrn\_measured\_fraction\_theta\_full Low ..... 0.955 Note

**Explanation:** The crystal selected for data collection was of poor quality which resulted in very weak diffraction intensity at high theta angles.

**Computational Details.** All calculations reported in the present study were performed via density functional theory (DFT) using the Gaussian 03 series of packages.<sup>11</sup> Attempts at optimization of clusters [TeFe<sub>3</sub>(CO)<sub>9</sub>Cu<sub>2</sub>(MeCN)<sub>2</sub>] and **1** led to the elongation of the Cu—Fe and Cu—Cu bonds, respectively, by more than 0.2 Å. Thus, to precisely calculate the natural charges<sup>12</sup> and Wiberg bond indices,<sup>13</sup> the single-point calculations of [TeFe<sub>3</sub>(CO)<sub>9</sub>Cu<sub>2</sub>(MeCN)<sub>2</sub>] and **1–4** with a PBE1PBE (PBE0)<sup>14</sup> hybrid functional and the large basis set Def2-TZVP<sup>15</sup> were carried out by using the Weinhold NBO method<sup>16</sup> based on their single-crystal diffraction data. Graphical representations of the molecular orbitals were obtained using GaussView 5.0 software. For orbital contributions, the molecular orbital compositions were analyzed using the AOMix program.<sup>17</sup>

## References

- (1) D. F. Shriver and M. A. Drezdon, *The Manipulation of Air-Sensitive Compounds*, Wiley-VCH Publisher, New York, 1986.
- (2) R. E. Bachman and K. H. Whitmire, *Inorg. Chem.*, 1994, **33**, 2527–2533.
- (3) G. J. Kubas, *Inorg. Synth.*, 1979, **19**, 90–92.
- (4) M. Shieh, C.-H. Ho, W.-S. Sheu, B.-G. Chen, Y.-Y. Chu, C.-Y. Miu, H.-L. Liu and C.-C. Shen, *J. Am. Chem. Soc.*, 2008, **130**, 14114–14116.
- (5) C. Tubaro, A. Biffis, R. Gava, E. Scattolin, A. Volpe, M. Basato, M. M. Díaz-Requejo and P. J. Perez, *Eur. J. Org. Chem.*, 2012, 1367–1372.
- (6) (a) W. A. Herrmann, C. Köcher, L. J. Gooßen and G. R. J. Artus, *Chem.—Eur. J.*, 1996, **2**, 1627–1636; (b) Q. Liu, F. van Rantwijk and R. A. Sheldon, *J. Chem. Technol. Biotechnol.*, 2006, **81**, 401–405; (c) F. M. Nachtigall, Y. E. Corilo, C. C. Cassol, G. Ebeling, N. H. Morgan, J. Dupont and M. N. Eberlin, *Angew. Chem., Int. Ed.*, 2008, **47**, 151–154.
- (7) (a) X. Xue, X.-S. Wang, R.-G. Xiong, X.-Z. You, B. F. Abrahams, C.-M. Che and H.-X. Ju, *Angew. Chem., Int. Ed.*, 2002, **41**, 2944–2946; (b) M. Scheer, A. Schindler, R. Merkle, B. P. Johnson, M. Linseis, R. Winter, C. E. Anson and A. V. Virovets, *J. Am. Chem. Soc.*, 2007, **129**, 13386–13387; (c) M. S. Doescher, J. M. Tour, A. M. Rawlett and M. L. Myrick, *J. Phys. Chem. B*, 2001, **105**, 105–110; (d) H. Hagenström, M. A.

Schneeweiss and D. M. Kolb, *Langmuir*, 1999, **15**, 7802–7809.

- (8) (a) A. J. Bard and L. R. Faulkner, *Electrochemical Methods: Fundamentals and Applications*, 2nd ed., Wiley, New York, 2001, pp 291; (b) T. Nakanishi, H. Murakami, T. Sagara and N. Nakashima, *J. Phys. Chem. B*, 1999, **103**, 304.
- (9) G. M. Sheldrick, *SADABS*, Bruker AXS Inc., Madison, Wisconsin, USA, 2003.
- (10) G. M. Sheldrick, *SHELXL97*, version 97-2; University of Göttingen, Germany, 1997.
- (11) M. J. Frisch, G. W. Trucks, H. B. Schlegel, G. E. Scuseria, M. A. Robb, J. R. Cheeseman, J. A. Montgomery, Jr., T. Vreven, K. N. Kudin, J. C. Burant, J. M. Millam, S. S. Iyengar, J. Tomasi, V. Barone, B. Mennucci, M. Cossi, G. Scalmani, N. Rega, G. A. Petersson, H. Nakatsuji, M. Hada, M. Ehara, K. Toyota, R. Fukuda, J. Hasegawa, M. Ishida, T. Nakajima, Y. Honda, O. Kitao, H. Nakai, M. Klene, X. Li, J. E. Knox, H. P. Hratchian, J. B. Cross, V. Bakken, C. Adamo, J. Jaramillo, R. Gomperts, R. E. Stratmann, O. Yazyev, A. J. Austin, R. Cammi, C. Pomelli, J. W. Ochterski, P. Y. Ayala, K. Morokuma, G. A. Voth, P. Salvador, J. J. Dannenberg, V. G. Zakrzewski, S. Dapprich, A. D. Daniels, M. C. Strain, O. Farkas, D. K. Malick, A. D. Rabuck, K. Raghavachari, J. B. Foresman, J. V. Ortiz, Q. Cui, A. G. Baboul, S. Clifford, J. Cioslowski, B. B. Stefanov, G. Liu, A. Liashenko, P. Piskorz, I. Komaromi, R. L. Martin, D. J. Fox, T. Keith, M. A. Al-Laham, C. Y. Peng, A. Nanayakkara, M. Challacombe, P. M. W. Gill, B. Johnson, W. Chen, M. W. Wong, C. Gonzalez and J. A.

Pople, GAUSSIAN 03 (Revision E.01), Gaussian, Inc., Wallingford, CT, 2004.

- (12) (a) A. E. Reed and F. Weinhold, *J. Chem. Phys.*, 1983, **78**, 4066–4073; (b) A. E. Reed, R. B. Weinstock and F. Weinhold, *J. Chem. Phys.*, 1985, **83**, 735–746.
- (13) K. B. Wiberg, *Tetrahedron*, 1968, **24**, 1083–1096.
- (14) C. Adamo and V. Barone, *J. Chem. Phys.*, 1999, **110**, 6158–6170.
- (15) F. Weigend and R. Ahlrichs, *Phys. Chem. Chem. Phys.*, 2005, **7**, 3297–3305.
- (16) A. E. Reed, L. A. Curtiss and F. Weinhold, *Chem. Rev.*, 1988, **88**, 899–926.
- (17) S. I. Gorelsky, AOMIX program, <http://www.sg-chem.net/>.
- (18) R. B. N. Baig and R. S. Varma, *Green Chem.*, 2013, **15**, 398–417.
- (19) A. S. Demir, Ö. Reis and M. Emrullahoglu, *J. Org. Chem.*, 2003, **68**, 10130–10134.
- (20) R. Luque, B. Baruwati and R. S. Varma, *Green Chem.*, 2010, **12**, 1540–1543.
- (21) N. Hussain, P. Gogoi, V. K. Azhaganand, M. V. Shelke and M. R. Das, *Catal. Sci. Technol.*, 2015, **5**, 1251–1260.
- (22) C. González-Arellano, A. Corma, M. Iglesias and F. Sánchez, *Chem. Commun.*, 2005, 1990–1992.
- (23) X. Zhang, H. Zhao and J. Wang, *J. Nanosci. Nanotechnol.*, 2010, **10**, 5153–5160.
- (24) A. Prastaro, P. Ceci, E. Chiancone, A. Boffi, G. Fabrizi and S. Cacchi, *Tetrahedron Lett.*, 2010, **51**, 2550–2552.
- (25) M. S. Wong and X. L. Zhang, *Tetrahedron Lett.*, 2001, **42**, 4087–4089.

- (26) G. W. Kabalka and L. Wang, *Tetrahedron Lett.*, 2002, **43**, 3067–3068.
- (27) A. L., II. Miller and N. B. Bowden, *J. Org. Chem.*, 2009, **74**, 4834–4840.
- (28) P. Puthiaraj, P. Suresh and K. Pitchumani, *Green Chem.*, 2014, **16**, 2865–2875.
- (29) N. Kirai and Y. Yamamoto, *Eur. J. Org. Chem.*, 2009, 1864–1867.
- (30) A. R. Kapdi, G. Dhangar, J. L. Serrano, J. A. De Haro, P. Lozano and I. J. S. Fairlamb, *RSC Adv.*, 2014, **4**, 55305–55312
- (31) G. Cheng and M. Luo, *Eur. J. Org. Chem.*, 2011, 2519–2523.

**Table S1** [TeFe<sub>3</sub>(CO)<sub>9</sub>Cu<sub>2</sub>(MeCN)<sub>2</sub>]- and **1–4**-catalyzed homocoupling of 4-bromophenylboronic acid: the optimization of the reaction conditions.<sup>a</sup>

The reaction scheme shows the conversion of compound 2 (4-bromophenylboronic acid) to a dimer. Compound 2 is a biphenyl system where the para position of one ring is substituted with a bromine atom and the para position of the other ring is substituted with a boronic acid group (-B(OH)<sub>2</sub>). An arrow labeled "Catalyst, Solvent" above and "Temperature, Oxidant" below points to the product, which is 4,4'-dibromo-4,4'-diphenylbiphenyl, where two biphenyl units are linked by a central carbon atom that is also bonded to two bromine atoms.

Entry	Catalyst	Solvent	Cu (mol%)	Temp. (°C)	Time (h)	Oxidant	Yield (%) <sup>b,c</sup>
1	[TeFe <sub>3</sub> (CO) <sub>9</sub> Cu <sub>2</sub> (Me <sub>2</sub> Im) <sub>2</sub> ] ( <b>1</b> )	MeOH	2.0	25	2	Air	84
2	–	MeOH	0	25	20	Air	0
3	–	MeOH	0	25	20	O <sub>2</sub> <sup>e</sup>	0
4	[TeFe <sub>3</sub> (CO) <sub>9</sub> Cu <sub>2</sub> (Me <sub>2</sub> Im) <sub>2</sub> ] ( <b>1</b> )	MeOH	2.0	25	8	— <sup>f</sup>	0
5	[Et <sub>4</sub> N] <sub>2</sub> [TeFe <sub>3</sub> (CO) <sub>9</sub> ]	MeOH	0 <sup>d</sup>	25	12	O <sub>2</sub> <sup>e</sup>	0
6	[TeFe <sub>3</sub> (CO) <sub>9</sub> Cu <sub>2</sub> (Me <sub>2</sub> Im) <sub>2</sub> ] ( <b>1</b> )	EtOH	2.0	25	24	Air	26
7	[TeFe <sub>3</sub> (CO) <sub>9</sub> Cu <sub>2</sub> (Me <sub>2</sub> Im) <sub>2</sub> ] ( <b>1</b> )	iPrOH	2.0	25	24	Air	Trace <sup>g</sup>
8	[TeFe <sub>3</sub> (CO) <sub>9</sub> Cu <sub>2</sub> (Me <sub>2</sub> Im) <sub>2</sub> ] ( <b>1</b> )	THF	2.0	25	24	Air	Trace <sup>g</sup>
9	[TeFe <sub>3</sub> (CO) <sub>9</sub> Cu <sub>2</sub> (Me <sub>2</sub> Im) <sub>2</sub> ] ( <b>1</b> )	DMF	2.0	25	24	Air	60
10	[TeFe <sub>3</sub> (CO) <sub>9</sub> Cu <sub>2</sub> (Me <sub>2</sub> Im) <sub>2</sub> ] ( <b>1</b> )	MeOH	2.0	64	8	Air	27
11	[TeFe <sub>3</sub> (CO) <sub>9</sub> Cu <sub>2</sub> (Me <sub>2</sub> Im) <sub>2</sub> ] ( <b>1</b> )	MeOH	2.0	25	1	O <sub>2</sub> <sup>e</sup>	85
12	[TeFe <sub>3</sub> (CO) <sub>9</sub> Cu <sub>2</sub> (Me <sub>2</sub> Im) <sub>2</sub> ] ( <b>1</b> )	MeOH	1.0	25	2	O <sub>2</sub> <sup>e</sup>	88
13	[TeFe <sub>3</sub> (CO) <sub>9</sub> Cu <sub>2</sub> (Me <sub>2</sub> Im) <sub>2</sub> ] ( <b>1</b> )	MeOH	0.5	25	12	O <sub>2</sub> <sup>e</sup>	82
14	[TeFe <sub>3</sub> (CO) <sub>9</sub> Cu <sub>2</sub> (MeImCH <sub>2</sub> ImMe)] ( <b>2</b> )	MeOH	1.0	25	2	O <sub>2</sub> <sup>e</sup>	87
15	[TeFe <sub>3</sub> (CO) <sub>9</sub> Cu <sub>2</sub> (MeIm(CH <sub>2</sub> ) <sub>2</sub> ImMe)] ( <b>3</b> )	MeOH	1.0	25	2	O <sub>2</sub> <sup>e</sup>	88
16	[TeFe <sub>3</sub> (CO) <sub>9</sub> Cu <sub>2</sub> (MeIm(CH <sub>2</sub> ) <sub>3</sub> ImMe)] ( <b>4</b> )	MeOH	1.0	25	2	O <sub>2</sub> <sup>e</sup>	88
17	[TeFe <sub>3</sub> (CO) <sub>9</sub> Cu <sub>2</sub> (MeCN) <sub>2</sub> ]	MeOH	1.0	25	3	O <sub>2</sub> <sup>e</sup>	85
18	[TeFe <sub>3</sub> (CO) <sub>9</sub> Cu <sub>2</sub> (MeCN) <sub>2</sub> ]	MeOH	0.5	25	17	O <sub>2</sub> <sup>e</sup>	78

<sup>a</sup> Reaction conditions: 4-bromophenylboronic acid (1.0 mmol), solvent (3.0 mL). <sup>b</sup> Isolated yield as an average of three runs. <sup>c</sup> All reactions were monitored by TLC. <sup>d</sup> 3.0 mol% of Fe loading. <sup>e</sup> O<sub>2</sub> (1 atm, balloon). <sup>f</sup> N<sub>2</sub> atmosphere. <sup>g</sup> Detected by <sup>1</sup>H NMR.

**Table S2** The reported catalytic systems for homocoupling of 4-bromophenylboronic acid, in which higher temperature (Entries 1-8), additional base (Entries 1, 3, 5, 6, and 8-10), external additives (Entries 7-10), longer reaction time (Entries 5-14), and higher loading of the catalyst (Entries 2 and 8-14) are required compared to our system.

Entry	Catalyst	Additive	Base	Solvent	Oxidant	Temp. (°C)	Time (h)	Yield (%)	Reference
1	Nano-FGT <sup>a</sup>	—	0.1 N NaOH	H <sub>2</sub> O	—	120-130 (Microwave irradiation)	0.75-1	> 99	18
2	Cu(OAc) <sub>2</sub> (50.0 mol%)	—	—	DMF	O <sub>2</sub>	100	1	93	19
3	Nano-ferrite glutathione	—	0.1 M NaOH	H <sub>2</sub> O	—	120-130 (Microwave irradiation)	0.75	> 99	20
4	CuNP-rGO (25 mg mL <sup>-1</sup> )	—	—	DMF	—	Microwave irradiation (360 W)	0.25	92	21
5	Au-(MCM-41)	—	K <sub>2</sub> CO <sub>3</sub> (2 eq.)	Xylene	—	130	24	95	22
6	Au(I) PS- <i>co</i> -PMAA	—	Cs <sub>2</sub> CO <sub>3</sub>	1-methyl-pyrrolidin-2-one /H <sub>2</sub> O	—	110	43	99	23
7	Pd <sub>np</sub> /Te-Dps (0.05 mol%)	1 M Tris-HCl Buffer at PH 8.9	—	H <sub>2</sub> O	Air	100	24	78	24
8	Pd(OAc) <sub>2</sub> (5.0 mol%)	PPh <sub>3</sub>	K <sub>2</sub> CO <sub>3</sub> (2 eq.)	DMF	Air	90	4	12	25
9	PdCl <sub>2</sub> (3.0 mol%)	<i>p</i> -Toluenesulfonyl chloride	Na <sub>2</sub> CO <sub>3</sub> (2 eq.)	EtOH/H <sub>2</sub> O	— <sup>b</sup>	r.t.	12	96	26
10	PdCl <sub>2</sub> (3.0 mol%)	<i>p</i> -Toluenesulfonyl chloride	Na <sub>2</sub> CO <sub>3</sub> (2 eq.)	EtOH/H <sub>2</sub> O	Air	—	12	93	27
11	Cu(BDC) MOF (19.4 mol%)	—	—	DMF	Air	r.t.	16	93	28
12	[(phen)Cu(μ-OH) <sub>2</sub> Cl <sub>2</sub> ] • 3H <sub>2</sub> O (2.0 mol%)	—	—	IPA	Air	28	12	92	29
13	[Pd(Phbz)(OAc)(PPh <sub>3</sub> )] (5.0 mol%)	—	—	THF	Air	20	24	82	30
14	CuCl (2.0 mol%)	—	—	MeOH	Air	25	4	74	31

<sup>a</sup>Glutathione-functionalized nano-Fe<sub>3</sub>O<sub>4</sub>. <sup>b</sup> Under N<sub>2</sub>.

**Table S3** Results of natural bond order of  $[\text{TeFe}_3(\text{CO})_9\text{Cu}_2(\text{MeCN})_2]$  and **1–4** at the level of PBE0/Def2-TZVP.

Complex	Wiberg bond index					
	Te—Fe	Fe—Fe	Cu—Fe	Cu—X <sup>a</sup>	Cu—Cu	Te—Cu
$[\text{TeFe}_3(\text{CO})_9\text{Cu}_2(\text{MeCN})_2]$	0.616	0.160	0.079	0.200	0.028	
<b>1</b>	0.625	0.157	0.065	0.363	0.035	0.174
<b>2</b>	0.628	0.161	0.078	0.336	0.030	
<b>3</b>	0.626	0.158	0.066	0.366	0.034	0.208
<b>4</b>	0.626	0.159	0.068	0.354	0.029	0.182

<sup>a</sup> X = N or C atom.

**Table S4** Differential pulse voltammetry of  $[\text{TeFe}_3(\text{CO})_9\text{Cu}_2(\text{MeCN})_2]$  and **1–4**.

Complex	Oxidation process		Reduction process	
	$E_p^{\text{red}}/\text{V}^a$ ( $W_{1/2}/\text{mV}^c$ )	$E_p^{\text{ox}}/\text{V}^b$ ( $W_{1/2}/\text{mV}^c$ )	$E_p^{\text{red}}/\text{V}^a$ ( $W_{1/2}/\text{mV}^c$ )	$E_p^{\text{ox}}/\text{V}^b$ ( $W_{1/2}/\text{mV}^c$ )
$[\text{TeFe}_3(\text{CO})_9\text{Cu}_2(\text{MeCN})_2]$	0.054 (109)	— <sup>d</sup> (br)	-0.124 (105)	— <sup>d</sup> (br)
<b>1</b>	0.232 (118)	0.220 (95)	-0.464 (84)	-0.198 (98) <sup>e</sup>
	0.015 (113)	— <sup>d</sup> (br)	-0.085 (113)	— <sup>d</sup> (br)
<b>2</b>	0.277 (117)	0.263 (111)	-0.449 (97)	-0.337 (134) <sup>e</sup>
	0.134 (108)	— <sup>d</sup> (br)	-0.130 (105)	-0.174 (83)
<b>3</b>	0.286 (101)	0.274 (119)	-0.430 (111)	-0.398 (72) <sup>e</sup>
	0.097 (111)	0.083 (89)	-0.143 (99)	-0.193 (120)
<b>4</b>	0.265 (82)	0.255 (82)	-0.475 (115)	-0.489 (170) <sup>e</sup>
	0.060 (101)	— <sup>d</sup> (br)	-0.140 (103)	-0.148 (96)
$[\text{Cu}_2(\text{MeIm}(\text{CH}_2)_2\text{ImMe})_2][\text{PF}_6]_2$	0.242 (97)	0.232 (85)	-0.496 (104)	-0.380 (124) <sup>e</sup>
	0.399 (125)	0.363 (br)	-0.529 (50)	
$[\text{Cu}(\text{MeCN})_4][\text{BF}_4]$	0.517 (128)	— <sup>d</sup> (br)		-0.317 (166) <sup>e</sup>
	1.004 (119)	1.016 (132)	-0.600 (48)	
				-0.280 (106) <sup>e</sup>

<sup>a</sup>  $E_p^{\text{red}}$  = reductive peak potential. <sup>b</sup>  $E_p^{\text{ox}}$  = oxidative peak potential. <sup>c</sup>  $W_{1/2}$  = width at half-height. <sup>d</sup> Difficult to determine due to the Cu desorption. <sup>e</sup> The Cu desorption peak.

**Table S5** Crystallographic data for  $[TeFe_3(CO)_9Cu_2(Me_2Im)_2]$  (**1**),  $[TeFe_3(CO)_9Cu_2(MeImCH_2ImMe)]$  (**2**),  $[TeFe_3(CO)_9Cu_2(MeIm(CH_2)_2ImMe)]$  (**3**), and  $[TeFe_3(CO)_9Cu_2(MeIm(CH_2)_3ImMe)]$  (**4**).

	<b>1</b>	<b>2</b>	<b>3</b>	<b>4</b>
Empirical formula	C <sub>19</sub> H <sub>16</sub> Cu <sub>2</sub> Fe <sub>3</sub> N <sub>4</sub> O <sub>9</sub> Te	C <sub>18</sub> H <sub>12</sub> Cu <sub>2</sub> Fe <sub>3</sub> N <sub>4</sub> O <sub>9</sub> Te	C <sub>19</sub> H <sub>14</sub> Cu <sub>2</sub> Fe <sub>3</sub> N <sub>4</sub> O <sub>9</sub> Te	C <sub>20</sub> H <sub>16</sub> Cu <sub>2</sub> Fe <sub>3</sub> N <sub>4</sub> O <sub>9</sub> Te
Fw	866.59	850.55	864.57	878.60
Crystal system	Monoclinic	Orthorhombic	Triclinic	Triclinic
Space group	<i>C</i> 2/c	<i>Pnma</i>	<i>P</i> ī	<i>P</i> ī
Crystal dimens, mm	0.44 x 0.32 x 0.20	0.38 x 0.21 x 0.10	0.27 x 0.17 x 0.03	0.38 x 0.24 x 0.12
<i>a</i> , Å	32.1115(6)	16.6462(5)	9.9886(1)	10.1041(4)
<i>b</i> , Å	8.6471(2)	16.1627(5)	13.5547(2)	13.6572(5)
<i>c</i> , Å	21.3640(5)	9.3673(3)	20.5089(3)	20.2351(8)
$\alpha$ , deg			75.7093(7)	76.356(2)
$\beta$ , deg	116.247(1)		81.2285(6)	82.953(2)
$\gamma$ , deg			77.5563(7)	79.062(2)
<i>V</i> , Å <sup>3</sup>	5320.5(2)	2520.3(1)	2613.10(6)	2655.3(2)
Z	8	4	4	4
<i>D</i> (calcd), g cm <sup>-3</sup>	2.164	2.242	2.198	2.198
$\mu$ , mm <sup>-1</sup>	4.299	4.535	4.376	4.308
Color, habit	black, prism	black, prism	black, prism	black, prism
Diffractometer	Apex II CCD	Apex II CCD	Nonius (Kappa CCD)	Apex II CCD
Radiation ( $\lambda$ ), Å	0.71073	0.71073	0.71073	0.71073
Temperature, K	200(2)	200(2)	200(2)	200(2)
$\theta$ range for data collection, deg	1.96–25.02	2.45–25.02	2.06–25.02	1.56–25.07
$T_{\min}/T_{\max}$	0.25/0.48	0.28/0.66	0.42/0.64	0.29/0.63
No. of indep. reflns ( $I > 2 \sigma(I)$ )	4123 ( $R_{\text{int}} = 0.027$ )	1998 ( $R_{\text{int}} = 0.026$ )	7628 ( $R_{\text{int}} = 0.054$ )	7888 ( $R_{\text{int}} = 0.024$ )
No. of parameters	337	175	685	703
Goodness of fit	1.192	1.333	1.094	1.042
$R_1^a/wR_2^a$ ( $I > 2 \sigma(I)$ )	0.032/0.096	0.020/0.066	0.035/0.098	0.030/0.074
$R_1^a/wR_2^a$ (all data)	0.042/0.117	0.034/0.101	0.051/0.116	0.036/0.077

<sup>a</sup> The functions minimized during least-squares cycles were  $R_1 = \sum |F_o| - |F_c| / \sum |F_o|$  and  $wR_2 = \{\sum [w(F_o^2 - F_c^2)^2] / \sum [w(F_o^2)^2]\}^{1/2}$ .

**Table S6** Selected bond distances ( $\text{\AA}$ ) and bond angles (deg) for  $[\text{TeFe}_3(\text{CO})_9\text{Cu}_2(\text{Me}_2\text{Im})_2]$  (**1**),  $[\text{TeFe}_3(\text{CO})_9\text{Cu}_2(\text{MeImCH}_2\text{ImMe})]$  (**2**),  $[\text{TeFe}_3(\text{CO})_9\text{Cu}_2(\text{MeIm}(\text{CH}_2)_2\text{ImMe})]$  (**3**), and  $[\text{TeFe}_3(\text{CO})_9\text{Cu}_2(\text{MeIm}(\text{CH}_2)_3\text{ImMe})]$  (**4**).

<b>1</b>			
Te(1)—Fe(1)	2.5073(8)	Fe(2)—Cu(1)	2.5418(8)
Te(1)—Fe(2)	2.5118(8)	Fe(2)—Cu(2)	2.6348(9)
Te(1)—Fe(3)	2.4984(8)	Fe(1)—Fe(2)	2.7492(9)
Te(1)—Cu(2)	2.7818(7)	Fe(1)—Fe(3)	2.6409(9)
Cu(1)—Cu(2)	2.5949(9)	Fe(2)—Fe(3)	2.6498(9)
Fe(1)—Cu(1)	2.5434(8)	Cu(2)—C(15)	1.936(5)
Fe(1)—Cu(2)	2.5004(9)	Cu(1)—C(10)	1.929(5)
Te(1)—Fe(1)—Fe(2)	56.87(2)	Fe(1)—Fe(2)—Fe(3)	58.54(2)
Te(1)—Fe(1)—Fe(3)	57.99(2)	Fe(1)—Fe(3)—Fe(2)	62.61(2)
Te(1)—Fe(2)—Fe(1)	56.71(2)	Fe(2)—Fe(1)—Fe(3)	58.85(2)
Te(1)—Fe(2)—Fe(3)	57.82(2)	Fe(1)—Cu(1)—Cu(2)	58.23(2)
Te(1)—Cu(2)—Cu(1)	100.67(2)	Fe(1)—Cu(2)—Cu(1)	59.86(2)
Te(1)—Fe(3)—Fe(1)	58.32(2)	Fe(2)—Cu(1)—Cu(2)	61.71(2)
Te(1)—Fe(3)—Fe(2)	58.32(2)	Fe(2)—Cu(2)—Cu(1)	58.15(2)
Te(1)—Fe(1)—Cu(1)	110.13(3)	Fe(1)—Cu(1)—Fe(2)	65.45(3)
Te(1)—Fe(2)—Cu(1)	110.04(3)	Fe(1)—Cu(2)—Fe(2)	64.68(3)
Te(1)—Fe(1)—Cu(2)	67.49(2)	Cu(1)—Fe(1)—Cu(2)	61.92(3)
Te(1)—Fe(2)—Cu(2)	65.39(2)	Cu(1)—Fe(2)—Cu(2)	60.14(2)
Te(1)—Cu(2)—Fe(1)	56.37(2)	Fe(3)—Fe(1)—Cu(1)	103.17(3)
Te(1)—Cu(2)—Fe(2)	55.18(2)	Fe(2)—Fe(1)—Cu(1)	57.25(2)
Fe(2)—Cu(1)—Cu(2)	58.15(2)	Fe(3)—Fe(2)—Cu(1)	102.96(3)
Fe(1)—Te(1)—Cu(2)	56.14(2)	Fe(3)—Fe(2)—Cu(2)	108.47(3)
Fe(2)—Te(1)—Cu(2)	59.44(2)	Fe(1)—Fe(2)—Cu(2)	55.30(2)
Fe(3)—Te(1)—Cu(2)	108.48(2)	Fe(1)—Fe(2)—Cu(1)	57.30(2)
Fe(1)—Te(1)—Fe(2)	66.43(2)	Fe(2)—Fe(1)—Cu(2)	60.03(3)
Fe(1)—Te(1)—Fe(3)	63.69(2)	Fe(3)—Fe(1)—Cu(2)	113.00(3)
Fe(2)—Te(1)—Fe(3)	63.86(2)		
<b>2</b>			
Te(1)—Fe(1)	2.4651(6)	Te(1)—Fe(2)	2.4762(7)
Fe(1)—Cu(1)	2.4660(7)	Fe(2)—Cu(1)	2.5292(8)
Fe(1)—Fe(1a)	2.668(1)	Cu(1)—Cu(1a)	2.548(1)
Fe(1)—Fe(2)	2.7391(8)	Cu(1)—C(9)	1.939(4)

Te(1)–Fe(1)–Cu(1)	114.31(2)	Cu(1a)–Fe(2)–Fe(1)	85.77(3)
Te(1)–Fe(1)–Fe(1a)	57.24(1)	Te(1)–Fe(2)–Fe(1a)	56.14(2)
Cu(1)–Fe(1)–Fe(1a)	88.62(2)	Cu(1)–Fe(2)–Fe(1a)	85.77(3)
Te(1)–Fe(1)–Fe(2)	56.53(2)	Cu(1a)–Fe(2)–Fe(1a)	55.65(2)
Cu(1)–Fe(1)–Fe(2)	57.86(2)	Fe(1)–Fe(2)–Fe(1a)	58.28(3)
Fe(1a)–Fe(1)–Fe(2)	60.86(1)	Fe(1)–Cu(1)–Fe(2)	66.49(2)
Te(1)–Fe(2)–Cu(1)	111.71(3)	Fe(1)–Cu(1)–Cu(1a)	91.39(2)
Te(1)–Fe(2)–Cu(1a)	111.71(3)	Fe(2)–Cu(1)–Cu(1a)	59.75(1)
Cu(1)–Fe(2)–Cu(1a)	60.50(3)	Fe(1)–Te(1)–Fe(1a)	65.51(3)
Te(1)–Fe(2)–Fe(1)	56.14(2)	Fe(1)–Te(1)–Fe(2)	67.33(2)
Cu(1)–Fe(2)–Fe(1)	55.65(2)	Fe(1a)–Te(1)–Fe(2)	67.33(2)
<b>3</b>			
Te(1)–Fe(1)	2.4853(9)	Fe(3)–Cu(2)	2.521(1)
Te(1)–Fe(3)	2.5124(8)	Fe(2)–Cu(2)	2.588(1)
Te(1)–Fe(2)	2.5263(8)	Fe(1)–Fe(2)	2.644(1)
Te(1)–Cu(1)	2.6755(8)	Fe(1)–Fe(3)	2.660(1)
Fe(3)–Cu(1)	2.537(1)	Fe(2)–Fe(3)	2.751(1)
Fe(2)–Cu(1)	2.571(1)	Cu(1)–C(19)	1.928(5)
Cu(1)–Cu(2)	2.620(1)	Cu(2)–C(28)	1.939(6)
Fe(1)–Te(1)–Fe(3)	64.31(3)	Te(1)–Fe(1)–Fe(3)	58.34(2)
Fe(1)–Te(1)–Fe(2)	63.67(3)	Fe(2)–Fe(1)–Fe(3)	62.49(3)
Fe(3)–Te(1)–Fe(2)	66.19(3)	Te(1)–Fe(2)–Cu(1)	63.31(2)
Fe(1)–Te(1)–Cu(1)	110.25(3)	Te(1)–Fe(2)–Cu(2)	108.19(3)
Fe(3)–Te(1)–Cu(1)	58.45(2)	Cu(1)–Fe(2)–Cu(2)	61.03(3)
Fe(2)–Te(1)–Cu(1)	59.16(2)	Te(1)–Fe(2)–Fe(1)	57.41(3)
Fe(3)–Cu(1)–Fe(2)	65.18(3)	Cu(1)–Fe(2)–Fe(1)	108.61(3)
Fe(3)–Cu(1)–Cu(2)	58.50(3)	Cu(2)–Fe(2)–Fe(1)	104.21(4)
Fe(2)–Cu(1)–Cu(2)	59.81(3)	Te(1)–Fe(2)–Fe(3)	56.67(2)
Fe(3)–Cu(1)–Te(1)	57.56(2)	Cu(1)–Fe(2)–Fe(3)	56.81(3)
Fe(2)–Cu(1)–Te(1)	57.53(2)	Cu(2)–Fe(2)–Fe(3)	56.24(3)
Cu(2)–Cu(1)–Te(1)	102.95(3)	Fe(1)–Fe(2)–Fe(3)	59.04(3)
Fe(3)–Cu(2)–Fe(2)	65.15(3)	Te(1)–Fe(3)–Cu(2)	110.79(3)
Fe(3)–Cu(2)–Cu(1)	59.10(3)	Te(1)–Fe(3)–Cu(1)	63.99(3)
Fe(2)–Cu(2)–Cu(1)	59.16(3)	Fe(1)–Fe(3)–Fe(2)	58.46(3)
Te(1)–Fe(1)–Fe(2)	58.92(2)	Te(1)–Fe(3)–Fe(1)	57.35(3)
Te(1)–Fe(3)–Fe(2)	57.15(2)	Cu(1)–Fe(3)–Fe(1)	109.15(4)
Cu(1)–Fe(3)–Fe(2)	58.01(3)	Cu(2)–Fe(3)–Fe(2)	58.61(3)

---

Cu(2)–Fe(3)–Fe(1)	105.65(4)	<b>4</b>	
Te(1)–Fe(1)	2.5151(6)	Fe(3)–Cu(2)	2.5325(8)
Te(1)–Fe(2)	2.4874(6)	Cu(1)–Cu(2)	2.5817(7)
Te(1)–Fe(3)	2.4999(6)	Fe(1)–Fe(2)	2.6350(7)
Te(1)–Cu(1)	2.7929(5)	Fe(1)–Fe(3)	2.7865(8)
Fe(1)–Cu(1)	2.5165(7)	Fe(2)–Fe(3)	2.6451(8)
Fe(1)–Cu(2)	2.5797(8)	Cu(1)–C(19)	1.925(4)
Fe(3)–Cu(1)	2.5550(7)	Cu(2)–C(29)	1.944(4)
Te(1)–Fe(1)–Cu(1)	67.43(2)	Te(1)–Fe(3)–Fe(1)	56.51(2)
Te(1)–Fe(1)–Cu(2)	109.02(2)	Cu(2)–Fe(3)–Fe(1)	57.79(2)
Cu(1)–Fe(1)–Cu(2)	60.86(2)	Cu(1)–Fe(3)–Fe(1)	56.01 (2)
Te(1)–Fe(1)–Fe(2)	57.70(2)	Fe(2)–Fe(3)–Fe(1)	57.97(2)
Cu(1)–Fe(1)–Fe(2)	110.90(3)	Fe(1)–Cu(1)–Fe(3)	66.65(2)
Cu(2)–Fe(1)–Fe(2)	100.48(3)	Fe(1)–Cu(1)–Cu(2)	60.78(2)
Te(1)–Fe(1)–Fe(3)	55.99(2)	Fe(3)–Cu(1)–Cu(2)	59.08(2)
Cu(1)–Fe(1)–Fe(3)	57.34(2)	Fe(1)–Cu(1)–Te(1)	56.26 (2)
Cu(2)–Fe(1)–Fe(3)	56.16(2)	Fe(3)–Cu(1)–Te(1)	55.52(2)
Fe(2)–Fe(1)–Fe(3)	58.33(2)	Cu(2)–Cu(1)–Te(1)	100.97(2)
Te(1)–Fe(2)–Fe(1)	58.73(2)	Fe(3)–Cu(2)–Fe(1)	66.05(2)
Te(1)–Fe(2)–Fe(3)	58.20(2)	Fe(3)–Cu(2)–Cu(1)	59.94(2)
Fe(1)–Fe(2)–Fe(3)	63.71(2)	Fe(1)–Cu(2)–Cu(1)	58.36(2)
Te(1)–Fe(3)–Cu(2)	111.04(2)	Fe(2)–Te(1)–Fe(3)	64.06(2)
Te(1)–Fe(3)–Cu(1)	67.07(2)	Fe(2)–Te(1)–Fe(1)	63.57(2)
Cu(2)–Fe(3)–Cu(1)	60.99(2)	Fe(3)–Te(1)–Fe(1)	67.51(2)
Te(1)–Fe(3)–Fe(2)	57.74 (2)	Fe(2)–Te(1)–Cu(1)	106.82(2)
Cu(2)–Fe(3)–Fe(2)	101.45(3)	Fe(3)–Te(1)–Cu(1)	57.41(2)
Cu(1)–Fe(3)–Fe(2)	109.37(3)	Fe(1)–Te(1)–Cu(1)	56.31(2)

**Table S7** Electronic energy and cartesian coordinates of  $[\text{TeFe}_3(\text{CO})_9\text{Cu}_2(\text{Me}_2\text{Im})_2]$  (**1**) (PBE0/Def2-TZVP) (in gas).

$E = -11297.7735507$  a.u.

atomic symbol	x	y	z
C	-0.702010	4.435960	5.669820
C	1.824220	4.593340	5.704310
C	0.316500	5.497830	3.539090
C	2.198720	9.139990	5.049000
C	1.619510	9.246340	7.513140
C	3.210100	7.274810	6.794590
C	0.312800	7.296420	9.329630
C	1.828060	5.380230	8.425220
C	-0.844930	5.120810	8.421380
C	4.304020	6.174030	3.429870
C	3.745060	3.919730	2.544620
H	4.098980	3.325680	1.852900
H	2.814050	4.143690	2.335760
H	3.784950	3.470080	3.414540
C	5.620130	5.392330	1.789660
H	5.966490	4.820760	1.113270
C	6.098720	6.589950	2.134570
H	6.853590	7.032690	1.762840
C	5.441640	8.347050	3.786270
H	6.216920	8.810530	3.399210
H	5.588050	8.214750	4.746250
H	4.636240	8.885760	3.648310
C	0.740910	8.748270	2.234210
C	2.278630	7.390680	0.829680
H	2.751770	7.513470	-0.019160
H	1.680050	6.619360	0.760700
H	2.930360	7.235030	1.546320
C	1.449650	9.683890	0.312330
H	1.899210	9.798890	-0.517350
C	0.646790	10.558970	0.902500
H	0.418290	11.424550	0.584420
C	-0.700020	10.593560	3.021730
H	-0.952310	11.484210	2.699820

H	-0.251370	10.673980	3.889740
H	-1.501880	10.040150	3.117540
N	4.535790	5.138110	2.592520
N	5.279310	7.055170	3.138620
N	1.508280	8.577920	1.128600
N	0.207520	9.970970	2.065590
O	-1.400000	3.530610	5.880600
O	2.599770	3.772730	5.976400
O	0.175050	5.119080	2.460310
O	2.647260	9.979620	4.412840
O	1.644680	10.087710	8.289170
O	4.237330	6.922870	7.191230
O	0.236240	7.922470	10.278110
O	2.740520	4.799140	8.841020
O	-1.640520	4.391860	8.800780
Fe	0.480530	5.673710	5.318410
Fe	1.653130	7.965970	6.281840
Fe	0.412820	6.265430	7.891380
Cu	2.801570	6.434050	4.609820
Cu	0.661910	7.693500	3.855830
Te	-0.833080	7.618700	6.200510

**Table S8** Electronic energy and cartesian coordinates of [TeFe<sub>3</sub>(CO)<sub>9</sub>Cu<sub>2</sub>(MeImCH<sub>2</sub>ImMe)] (**2**) (PBE0/Def2-TZVP) (in gas).

E = -11257.0567454 a.u.

atomic symbol	x	y	z
C	15.728990	2.597350	4.075710
C	18.194300	2.340360	4.758590
C	16.416480	1.121690	6.331360
C	15.459330	5.383800	8.758430
C	13.591620	4.040680	7.590320
C	11.988590	0.339420	6.513080
H	11.257820	-0.307090	6.603950
H	12.078480	0.850160	7.344900
H	12.824230	-0.137380	6.331360
C	10.535380	1.213820	4.670540
H	9.816260	0.601250	4.772640
C	10.613620	2.204590	3.785330
H	9.962750	2.434100	3.130550
C	12.501300	2.243380	5.029300
C	12.261590	4.040680	3.337570
H	13.250380	4.040680	3.292610
H	11.917020	4.040680	2.409270
N	11.699280	1.247760	5.414300
N	11.821470	2.838170	4.002650
O	15.317830	2.459960	3.010650
O	19.168770	2.091450	4.198420
O	16.258340	0.087280	6.813770
O	15.474970	6.238800	9.514370
O	12.507950	4.040680	7.970640
Fe	16.679490	2.706930	5.586280
Fe	15.393240	4.040680	7.603530
Cu	14.220350	2.766570	5.760050
Te	17.850400	4.040680	7.297130
Cu	14.220350	5.314780	5.760050
N	11.821470	5.243180	4.002650
Fe	16.679490	5.374420	5.586280
C	15.459330	2.697550	8.758430
C	15.728990	5.484000	4.075710

C	16.416480	6.959660	6.331360
C	12.501300	5.837970	5.029300
C	10.613620	5.876760	3.785330
C	18.194300	5.740990	4.758590
O	15.474970	1.842550	9.514370
O	15.317830	5.621390	3.010650
O	16.258340	7.994070	6.813770
N	11.699280	6.833590	5.414300
C	10.535380	6.867530	4.670540
H	9.962750	5.647250	3.130550
O	19.168770	5.989900	4.198420
C	11.988590	7.741930	6.513080
H	9.816260	7.480100	4.772640
H	11.257820	8.388440	6.603950
H	12.078480	7.231190	7.344900
H	12.824230	8.218730	6.331360

**Table S9** Electronic energy and cartesian coordinates of [TeFe<sub>3</sub>(CO)<sub>9</sub>Cu<sub>2</sub>(MeIm(CH<sub>2</sub>)<sub>2</sub>ImMe)] (**3**) (PBE0/Def2-TZVP) (in gas).

E = -11296.7983211 a.u.

atomic symbol	x	y	z
Te	1.208800	9.157380	4.009490
Cu	2.834050	8.137230	5.873820
Cu	5.049800	7.701050	4.545840
Fe	2.369050	9.248390	1.813590
Fe	2.743630	7.224090	3.472230
Fe	3.649720	9.747070	4.091060
O	0.028320	8.483210	0.233220
O	2.346360	12.023240	0.923000
O	4.496500	8.311620	0.031620
O	4.978310	5.905530	2.110850
O	0.894340	5.781330	1.739280
O	2.208480	5.165990	5.488610
O	4.867110	10.204790	6.704130
O	3.156710	12.633820	3.986510
O	6.079980	9.775070	2.462660
N	1.801050	7.907540	8.645010
N	3.528350	6.701760	8.336680
N	6.850070	6.676680	6.654720
N	7.758410	6.486480	4.735580
C	0.955120	8.758410	0.843950
C	2.347870	10.942540	1.304460
C	3.662770	8.646860	0.755000
C	4.148170	6.493910	2.701810
C	1.620830	6.392930	2.397440
C	2.474210	6.056120	4.798830
C	4.319770	9.895410	5.727760
C	3.327110	11.501340	4.012200
C	5.118660	9.701780	3.089200
C	2.703830	7.579380	7.714100
C	0.717510	8.839790	8.425620
H	0.184660	8.920410	9.245850
H	0.148270	8.512920	7.698280
H	1.082780	9.715910	8.186470

C	2.040900	7.240120	9.842740
H	1.530940	7.303880	10.641220
C	3.141700	6.482620	9.643110
H	3.565080	5.914320	10.275580
C	4.679330	6.101670	7.688400
H	4.446150	5.879380	6.751560
H	4.911670	5.257790	8.150890
C	5.892600	7.028680	7.696310
H	5.591830	7.963040	7.561910
H	6.337190	6.976760	8.579780
C	8.083540	6.077890	6.850390
H	8.451880	5.805150	7.682470
C	8.653020	5.959150	5.670440
H	9.507850	5.585580	5.488610
C	8.037490	6.579790	3.300680
H	8.917440	6.190750	3.114890
H	8.030650	7.519750	3.027930
H	7.350040	6.089300	2.802610
C	6.639960	6.922250	5.336420

**Table S10** Electronic energy and cartesian coordinates of [TeFe<sub>3</sub>(CO)<sub>9</sub>Cu<sub>2</sub>(MeIm(CH<sub>2</sub>)<sub>3</sub>ImMe)] (**4**) (PBE0/Def2-TZVP) (in gas). E = -11335.9868279 a.u.

atomic symbol	x	y	z
C	9.144640	9.829650	5.803080
C	8.103300	11.401990	4.031390
C	9.907040	9.712710	3.174940
C	7.226340	10.711440	1.236660
C	5.886620	8.511310	0.872130
C	8.599730	8.396500	0.958360
C	6.344430	6.226400	2.665380
C	8.850070	6.283990	2.880960
C	7.232720	6.026960	5.077940
C	7.355670	7.698200	7.862870
C	4.888710	7.966590	7.815830
H	4.149120	7.831020	8.444940
H	4.747690	7.413240	7.020140
H	4.927270	8.911310	7.555170
C	6.237230	7.126580	9.744310
H	5.519400	6.983060	10.349900
C	7.514660	6.924410	9.973610
H	7.895120	6.599420	10.781070
C	9.626640	7.264330	8.729120
H	10.017020	6.927550	9.573810
H	9.949390	8.190190	8.588010
C	10.109900	6.336100	7.504220
H	9.906090	5.386770	7.696280
H	9.641300	6.596840	6.673250
C	11.525360	6.516470	7.351350
H	12.002920	5.964590	8.019660
H	11.756530	7.464660	7.514020
C	13.107580	5.409930	5.820720
H	13.575580	4.907720	6.477260
C	13.436040	5.546600	4.548780
H	14.179460	5.148520	4.111740
C	12.593920	6.886800	2.614420
H	13.359540	6.473590	2.163660

H	12.714020	7.858860	2.637940
H	11.771760	6.670420	2.126420
C	11.551130	6.743540	4.858440
N	6.148930	7.586790	8.456110
N	8.204980	7.267990	8.829460
N	11.957110	6.132300	6.004940
N	12.498760	6.376060	3.976510
O	9.743680	10.109030	6.764770
O	7.913820	12.531840	3.951030
O	10.860140	9.892270	2.544650
O	7.238120	11.755130	0.764920
O	5.001900	8.184100	0.230280
O	9.476400	8.000600	0.333170
O	5.617850	5.581950	2.049990
O	9.575360	5.627860	2.267340
O	7.012770	5.180340	5.807390
Fe	8.446490	9.673650	4.169750
Fe	7.236560	9.064290	1.889870
Fe	7.482700	7.119270	3.661370
Cu	7.677570	8.152260	6.012190
Cu	9.892100	7.669300	4.470980
Te	6.001700	9.113280	4.042280

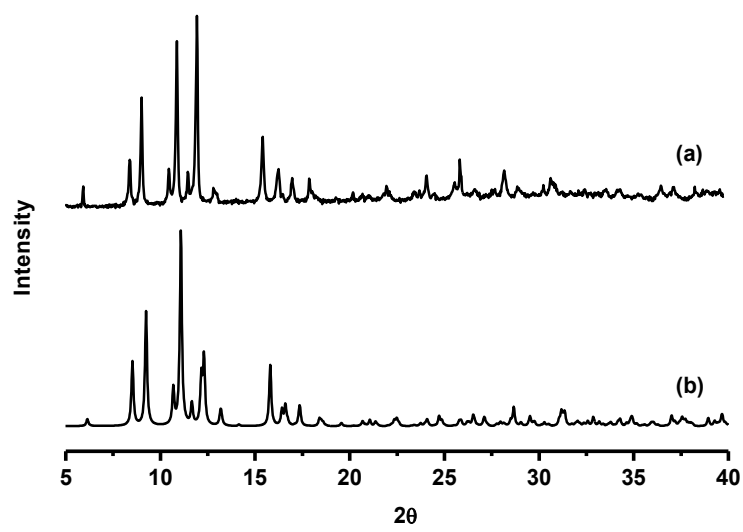


**Fig. S1** Powder X-ray diffraction (PXRD) patterns for (a) Crystals of **1** exposure to air for 10 days; (b) Calculated pattern for **1**.

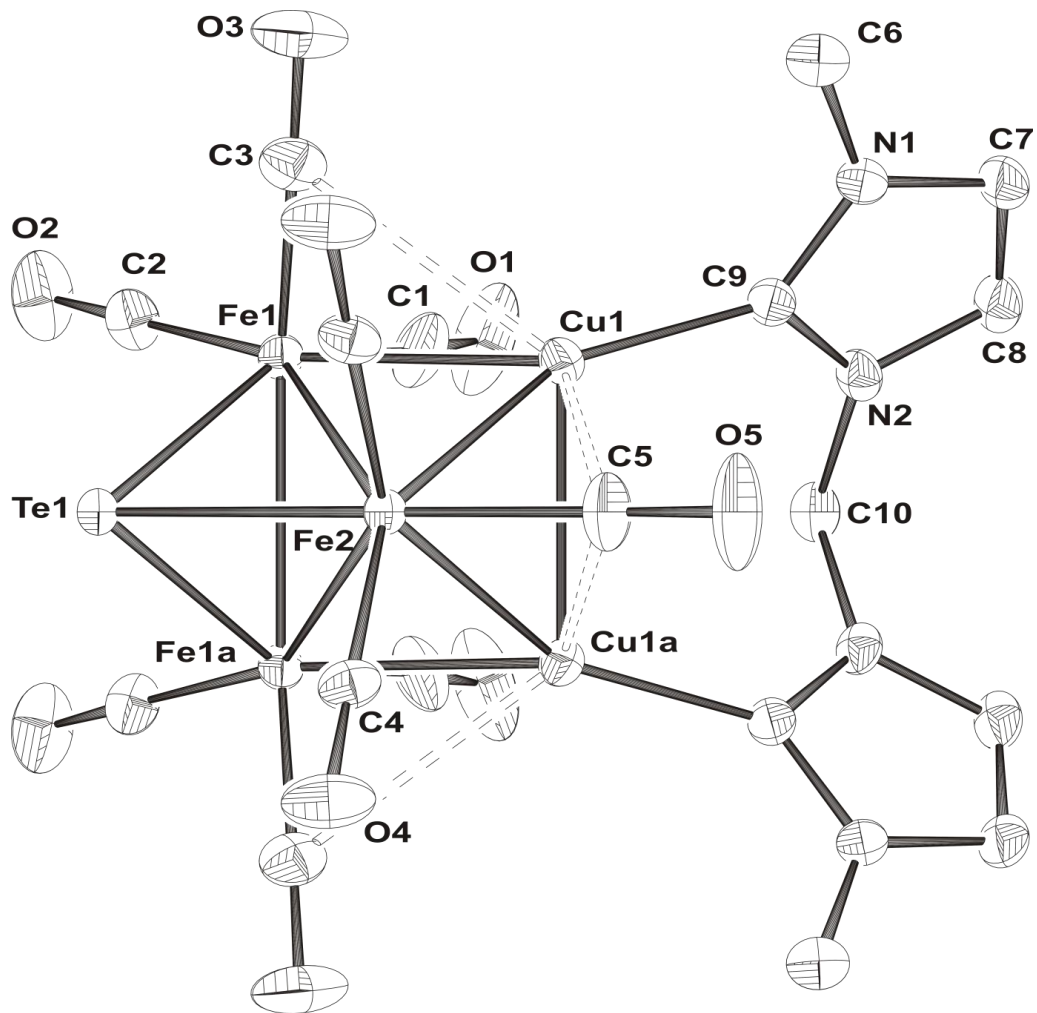


**Fig. S2** ORTEP of **2** at 30% probability and hydrogen atoms are omitted for clarity. The atoms with an additional label (a) are at the equivalent position ( $x, 1/2 - y, z$ ).

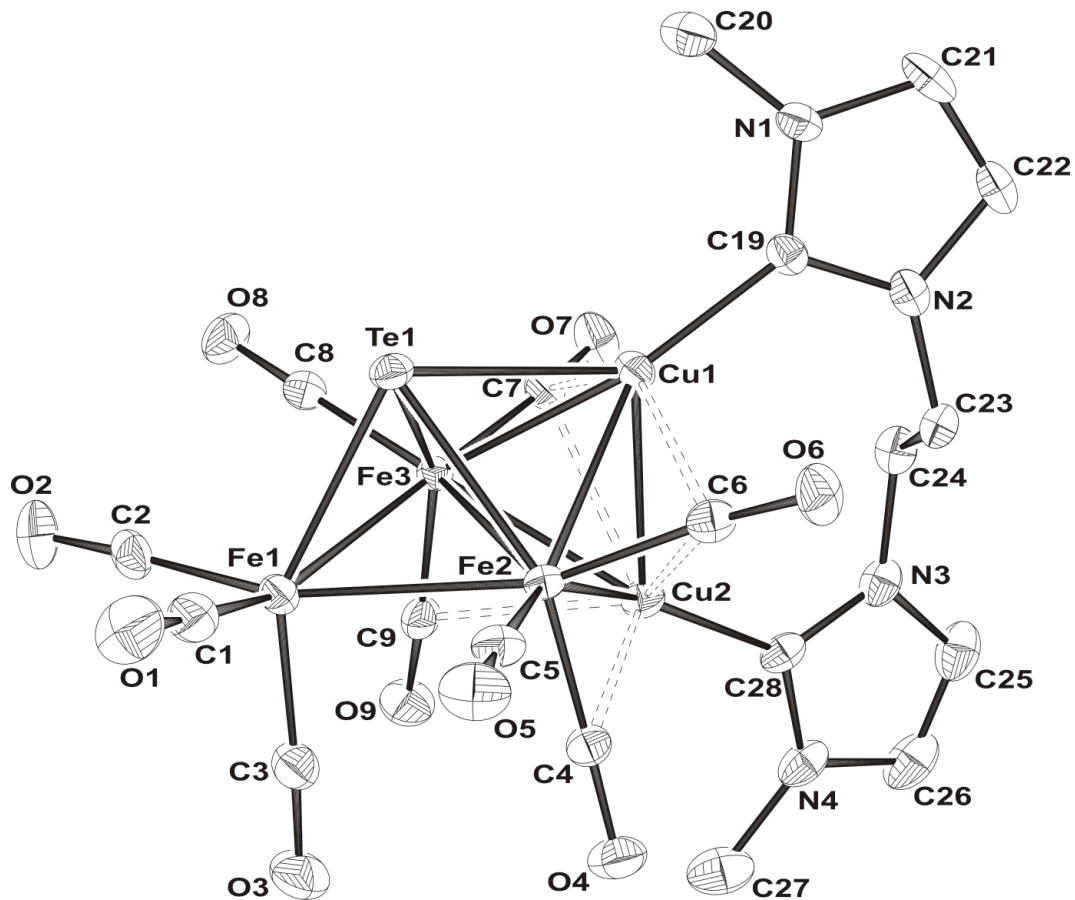


**Fig. S3** ORTEP of **3** at 30% probability and hydrogen atoms are omitted for clarity.

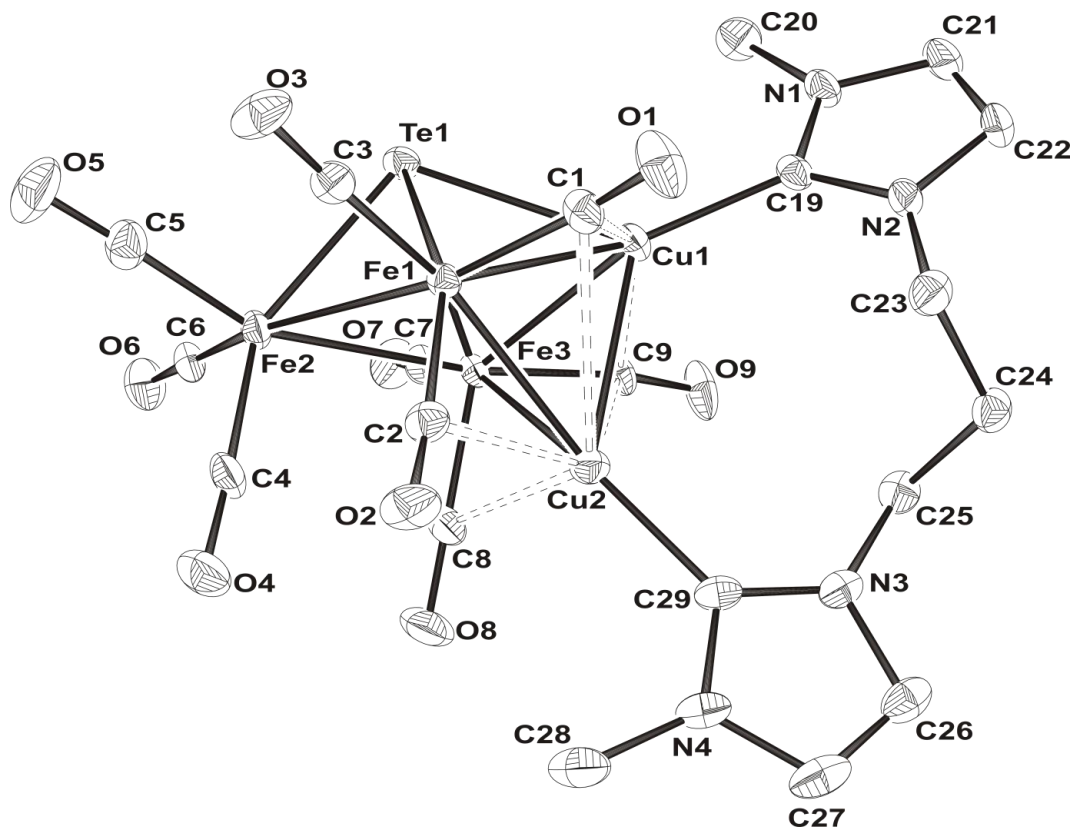


**Fig. S4** ORTEP of 4 at 30% probability and hydrogen atoms are omitted for clarity.

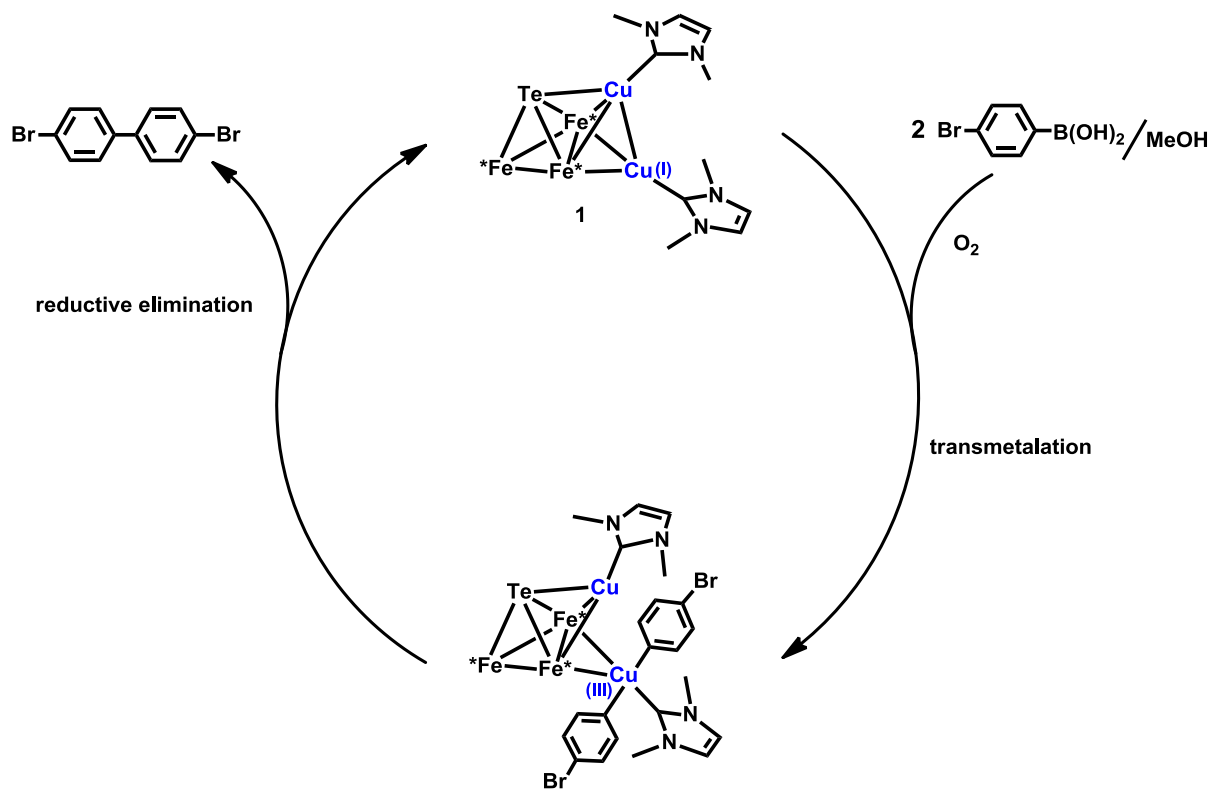


**Fig. S5** The proposed mechanism using the model complex **1** as the catalyst for the homocoupling of 4-bromophenylboronic acid to 4,4'-dibromobiphenyl.<sup>19,28</sup>

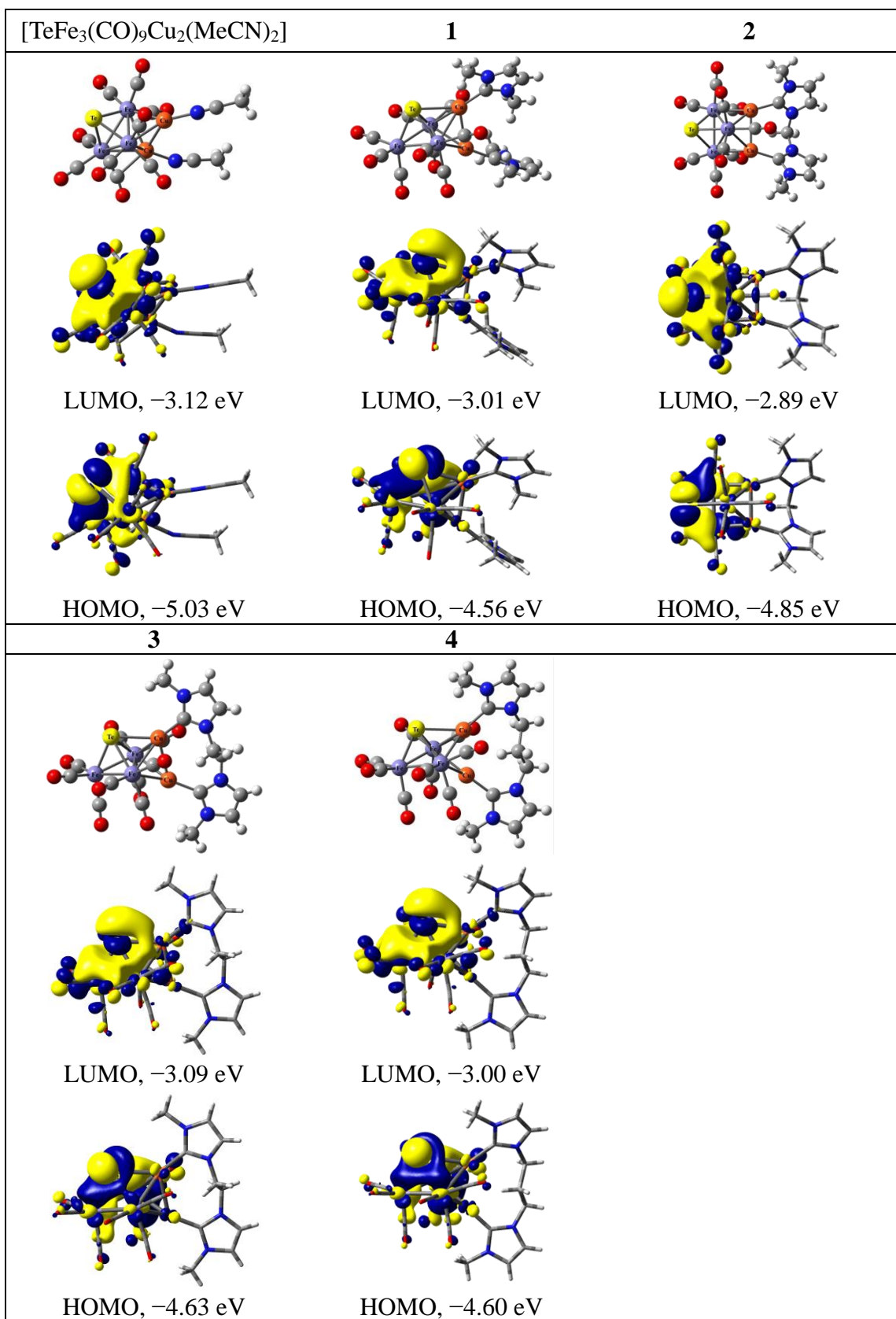


**Fig. S6** Spatial graphs (isovalue = 0.03) of the selected frontier molecular orbitals and their associated energies of [TeFe<sub>3</sub>(CO)<sub>9</sub>Cu<sub>2</sub>(MeCN)<sub>2</sub>] and **1–4**.

ArX <sup>a</sup>	Yield (%)	Product ratio	K <sub>Ar</sub> /K <sub>ArBr</sub>	log (K <sub>ArX</sub> /K <sub>ArBr</sub> )
p-BrC <sub>6</sub> H <sub>4</sub>	88	88/88	1	0
p-OMeC <sub>6</sub> H <sub>4</sub>	70	70/88	0.795	-0.100
p-NO <sub>2</sub> C <sub>6</sub> H <sub>4</sub>	99 <sup>b</sup>	99/88	1.125	0.051
m-BrC <sub>6</sub> H <sub>4</sub>	68	68/68	1	0
m-NO <sub>2</sub> C <sub>6</sub> H <sub>4</sub>	97	97/68	1.426	0.154

<sup>a</sup> X = substituents. <sup>b</sup> 78%/79% (based on 78% yield of 4,4'-dinitrobiphenyl and 21% yield of 4-nitrophenol).

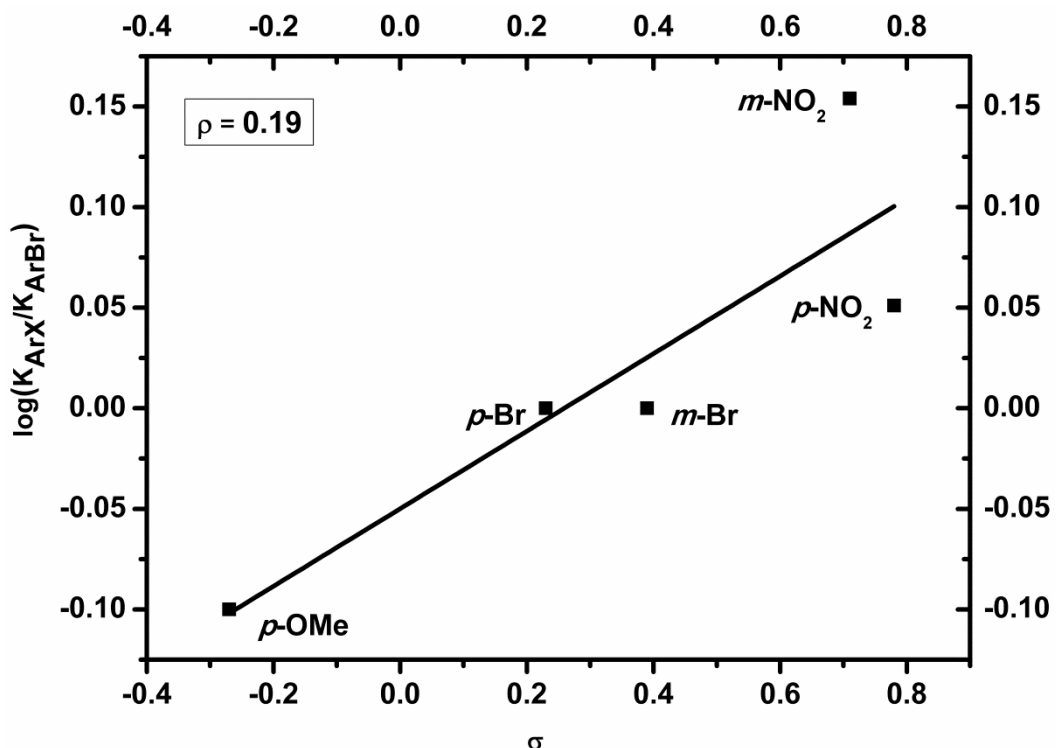
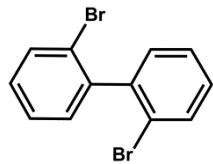


**Fig. S7** Correlation of product ratios with the Hammett equation.  $y = 0.19 x - 0.05$ ;  $R^2 = 0.70$ .

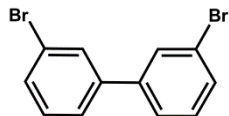
## Spectroscopic data of products

### 2,2'-dibromobiphenyl



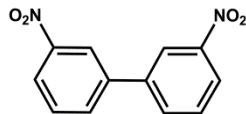
<sup>1</sup>H NMR (400 MHz, DMSO, ppm):  $\delta$  7.72 (dd, 2H,  $J$  = 7.6, 1.4 Hz), 7.46 (td, 2H,  $J$  = 7.6, 1.4 Hz), 7.35 (td, 2H,  $J$  = 7.6, 1.4 Hz), 7.28 (dd, 2H,  $J$  = 7.6, 1.4 Hz); <sup>13</sup>C NMR (100 MHz, DMSO, ppm):  $\delta$  141.95, 132.81, 131.52, 130.42, 128.15, 123.21

### 3,3'-dibromobiphenyl



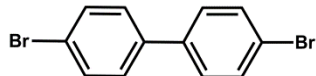
<sup>1</sup>H NMR (400 MHz, CDCl<sub>3</sub>, ppm):  $\delta$  7.71 (t, 2H,  $J$  = 1.8 Hz), 7.53–7.48 (m, 4H), 7.32 (t, 2H,  $J$  = 7.8 Hz); <sup>13</sup>C NMR (100 MHz, CDCl<sub>3</sub>, ppm):  $\delta$  141.82, 130.83, 130.39, 130.19, 125.75, 123.00

### 3,3'-dinitrobiphenyl



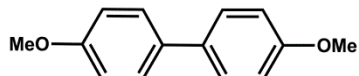
<sup>1</sup>H NMR (400 MHz, CDCl<sub>3</sub>, ppm):  $\delta$  8.50 (t, 2H,  $J$  = 1.8 Hz), 8.30 (m, 2H), 7.97 (m, 2H), 7.70 (t, 2H,  $J$  = 8.0 Hz); <sup>13</sup>C NMR (100 MHz, CDCl<sub>3</sub>, ppm):  $\delta$  148.90, 140.35, 133.07, 130.31, 123.31, 122.12

### 4,4'-dibromobiphenyl



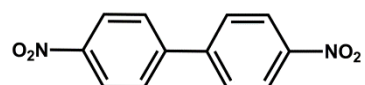
<sup>1</sup>H NMR (400 MHz, CDCl<sub>3</sub>, ppm):  $\delta$  7.56 (dd, 4H,  $J$  = 8.4 Hz), 7.41 (dd, 4H,  $J$  = 8.4 Hz); <sup>13</sup>C NMR (100 MHz, CDCl<sub>3</sub>, ppm):  $\delta$  138.93, 132.03, 128.52, 121.96

### 4,4'-dimethoxybiphenyl



<sup>1</sup>H NMR (400 MHz, CDCl<sub>3</sub>, ppm):  $\delta$  7.49 (dd, 4H,  $J$  = 8.6 Hz), 6.97 (dd, 4H,  $J$  = 8.6 Hz), 3.85 (s, 6H); <sup>13</sup>C NMR (100 MHz, CDCl<sub>3</sub>, ppm):  $\delta$  158.71, 133.51, 127.73, 114.17, 55.35

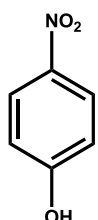
**4,4'-dinitrobiphenyl**



$^1\text{H}$  NMR (400 MHz,  $\text{CDCl}_3$ , ppm):  $\delta$  8.38 (dd, 4H,  $J = 8.8$  Hz), 7.80 (dd, 4H,  $J = 8.8$  Hz);

$^{13}\text{C}$  NMR (100 MHz,  $\text{CDCl}_3$ , ppm):  $\delta$  148.10, 144.99, 128.33, 124.39

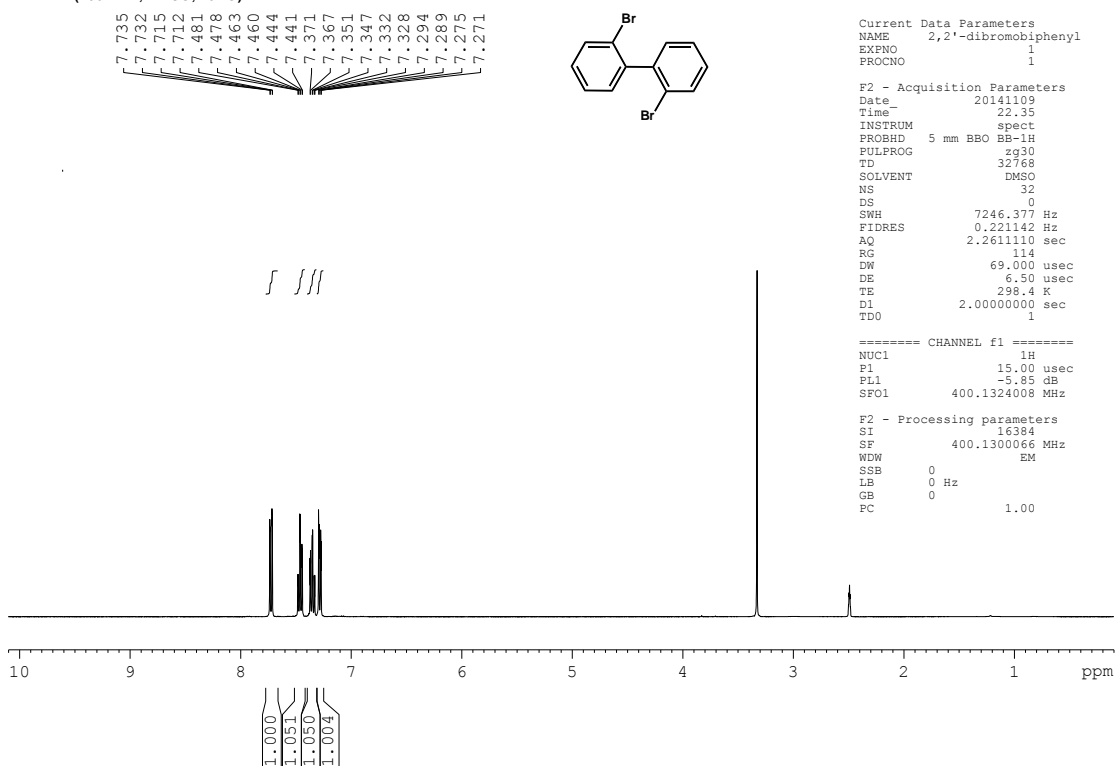
**4-nitrophenol**



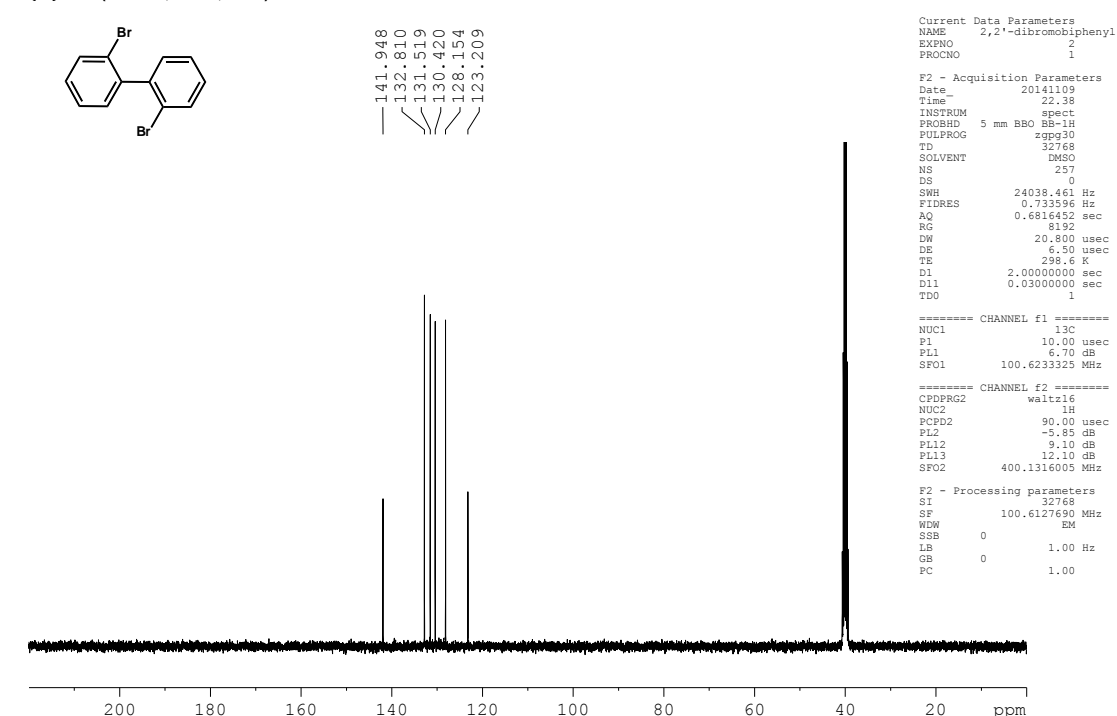
$^1\text{H}$  NMR (400 MHz,  $\text{CDCl}_3$ , ppm):  $\delta$  8.17 (dd, 2H,  $J = 9.2$  Hz), 6.90 (dd, 2H,  $J = 9.2$  Hz),

5.93 (s, 1H);  $^{13}\text{C}$  NMR (100 MHz,  $\text{CDCl}_3$ , ppm):  $\delta$  161.82, 141.39, 126.38, 115.83

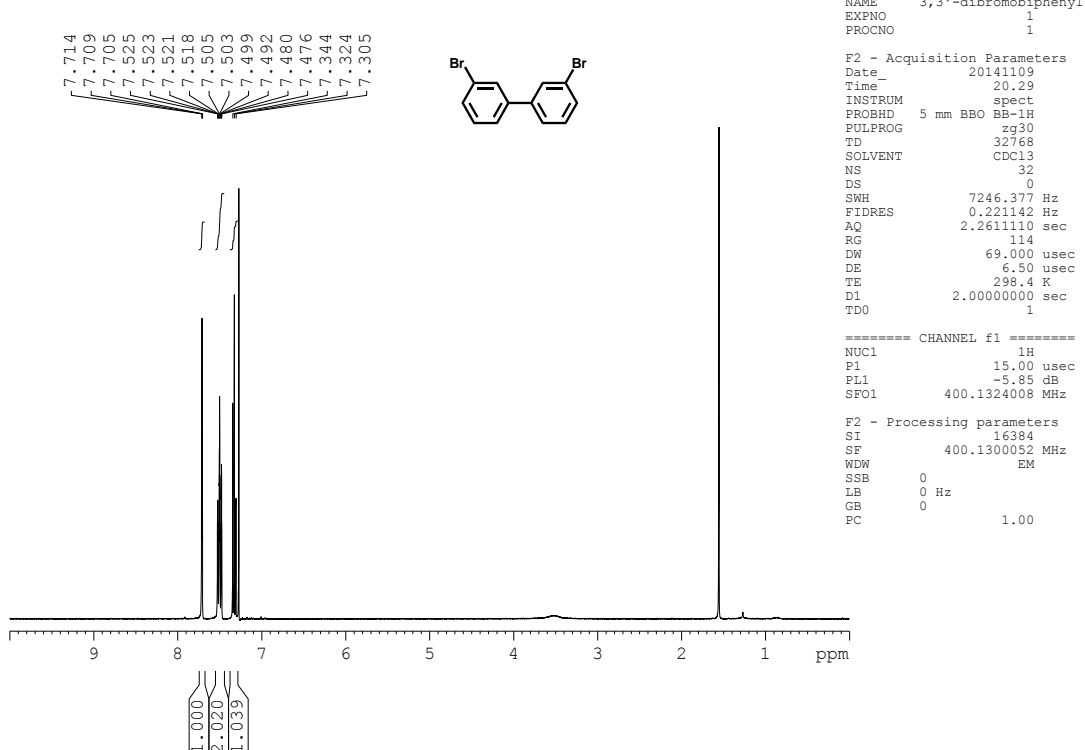
<sup>1</sup>H NMR (400 MHz, DMSO, 25 °C)



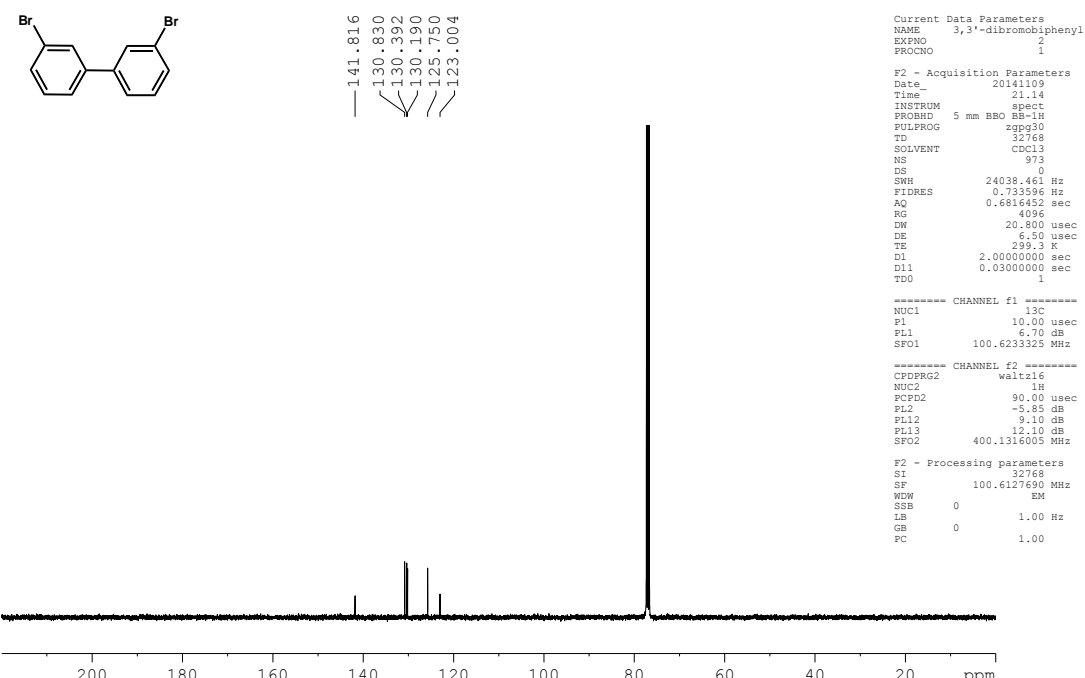
<sup>13</sup>C{<sup>1</sup>H} NMR (100 MHz, DMSO, 25 °C)



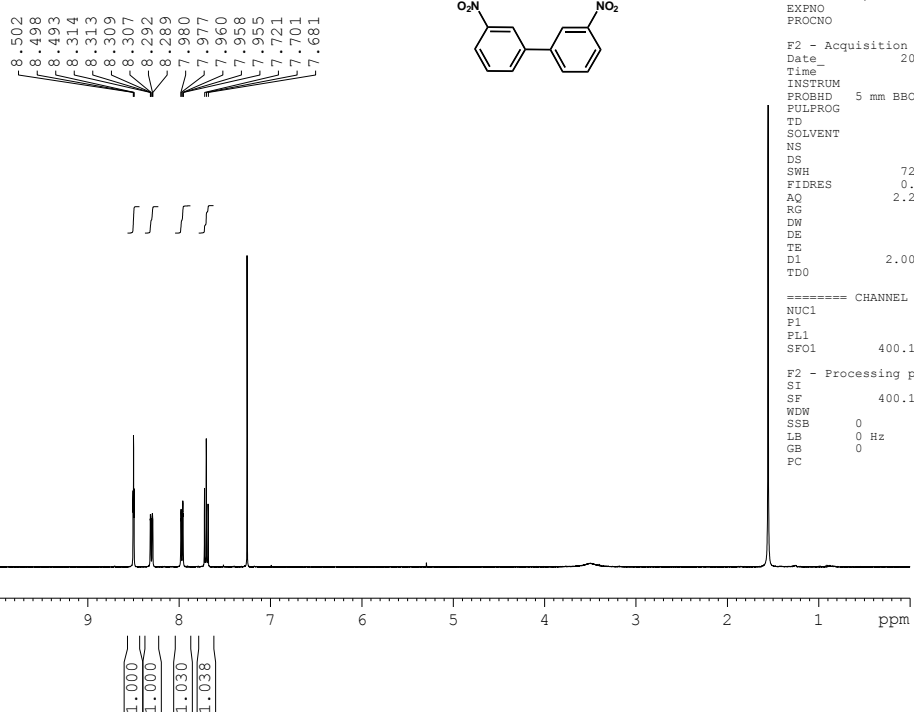
<sup>1</sup>H NMR (400 MHz, CDCl<sub>3</sub>, 25 °C)



<sup>13</sup>C({<sup>1</sup>H}) NMR (100 MHz, CDCl<sub>3</sub>, 25 °C)



<sup>1</sup>H NMR (400 MHz, CDCl<sub>3</sub>, 25 °C)



Current Data Parameters  
NAME 3,3'-dinitrobiphenyl  
EXPNO 1  
PROCNO 1

F2 - Acquisition Parameters

Date 20141215  
Time 23.35  
INSTRUM spect  
PROBHD 5 mm BBO BB-1H  
PULPROG zg30  
TD 32768  
SOLVENT CDCl<sub>3</sub>  
NS 32  
DS 0  
SWH 7246.377 Hz  
FIDRES 0.221142 Hz  
AQ 2.261110 sec  
RG 114  
DW 69.000 usec  
DE 6.50 usec  
TE 298.2 K  
D1 2.0000000 sec  
TDO 1 sec

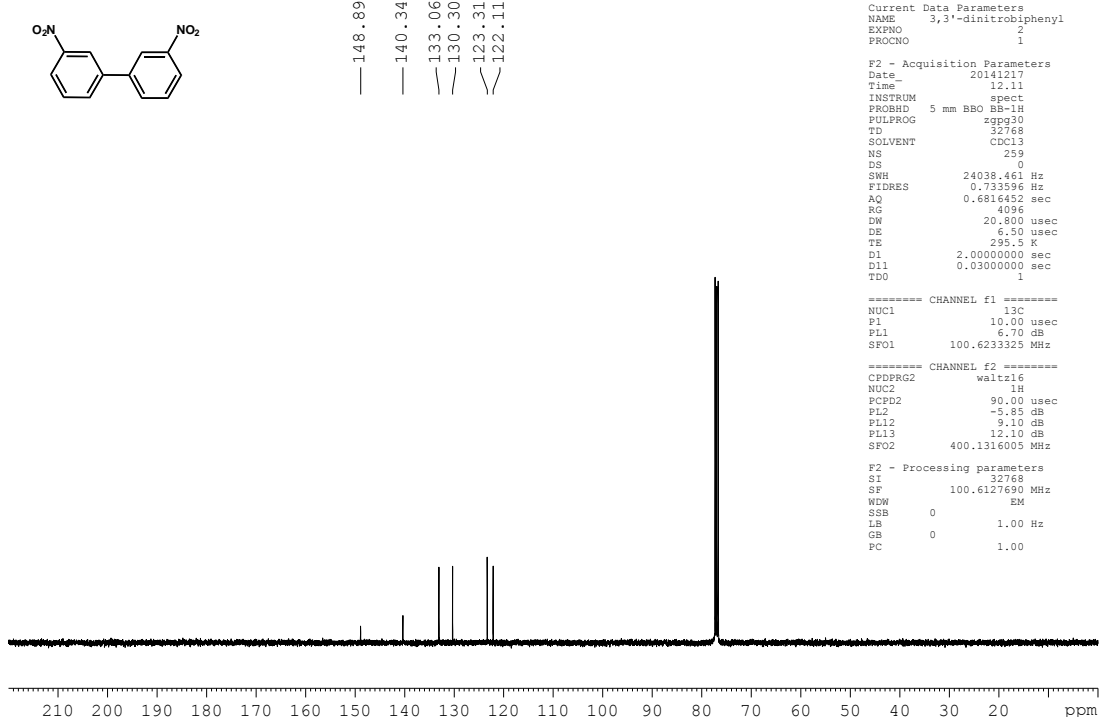
===== CHANNEL f1 =====

NUC1 <sup>1</sup>H  
P1 15.00 usec  
PL1 -5.85 dB  
SFO1 400.1324008 MHz

F2 - Processing parameters

SI 16384  
SF 400.1300118 MHz  
NDW EM  
SSB 0  
LB 0 Hz  
GB 0  
PC 1.00

<sup>13</sup>C(<sup>1</sup>H) NMR (100 MHz, CDCl<sub>3</sub>, 25 °C)



Current Data Parameters  
NAME 3,3'-dinitrobiphenyl  
EXPNO 2  
PROCNO 1

F2 - Acquisition Parameters

Date 20141215  
Time 12.11  
INSTRUM spect  
PROBHD 5 mm BBO BB-1H  
PULPROG zg30  
TD 32768  
SOLVENT CDCl<sub>3</sub>  
NS 259  
DS 0  
SWH 24038.461 Hz  
FIDRES 0.733596 Hz  
AQ 0.6816452 sec  
RG 4096  
DW 20.800 usec  
DE 6.70 usec  
TE 295.5 K  
D1 2.0000000 sec  
D11 0.0300000 sec  
TDO 1 sec

===== CHANNEL f1 =====

NUC1 <sup>13</sup>C  
P1 10.00 usec  
PL1 6.70 dB  
SFO1 100.6233325 MHz

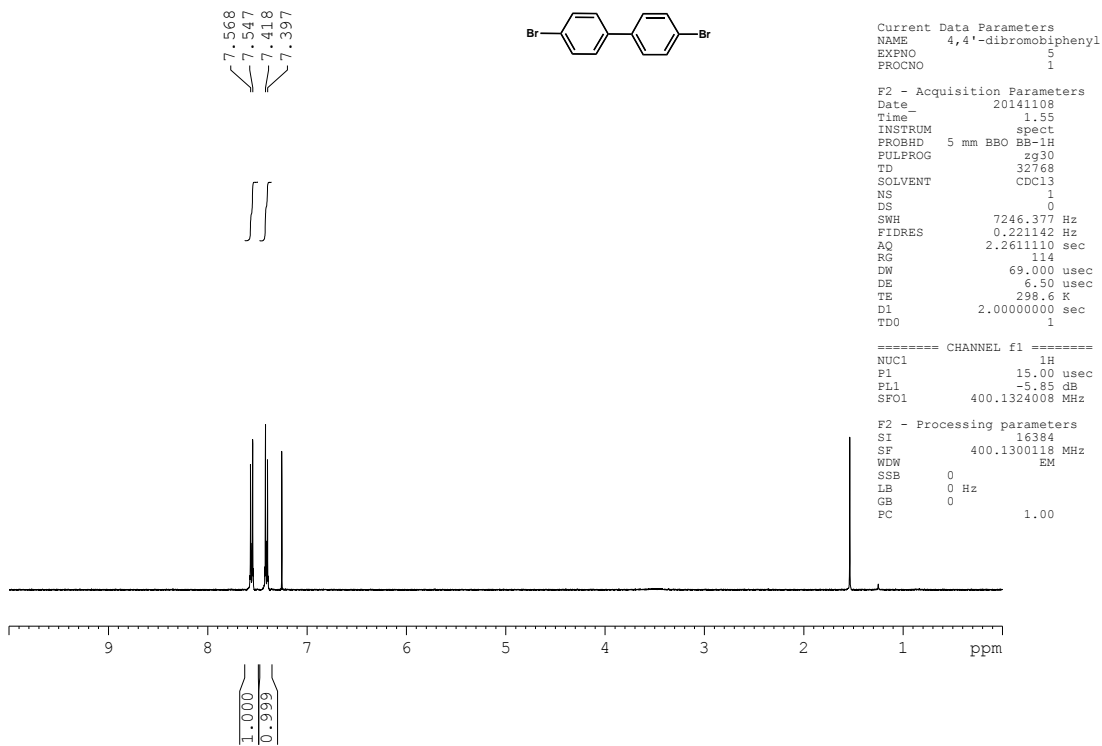
===== CHANNEL f2 =====

CPDPGR2 waltz16  
NUC2 <sup>1</sup>H  
PCPGR2 90.000 usec  
PL2 -5.85 dB  
PL12 9.10 dB  
PL13 12.10 dB  
SFO2 400.1316005 MHz

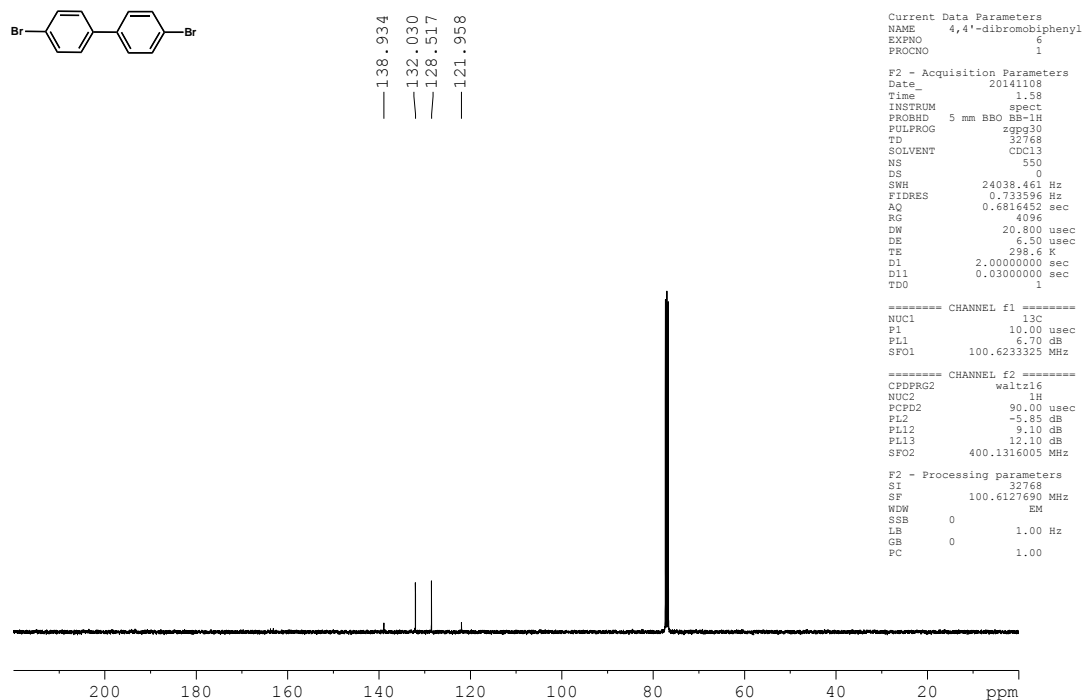
F2 - Processing parameters

SI 32768  
SF 100.6127690 MHz  
NDW EM  
SSB 0  
LB 1.00 Hz  
GB 0  
PC 1.00

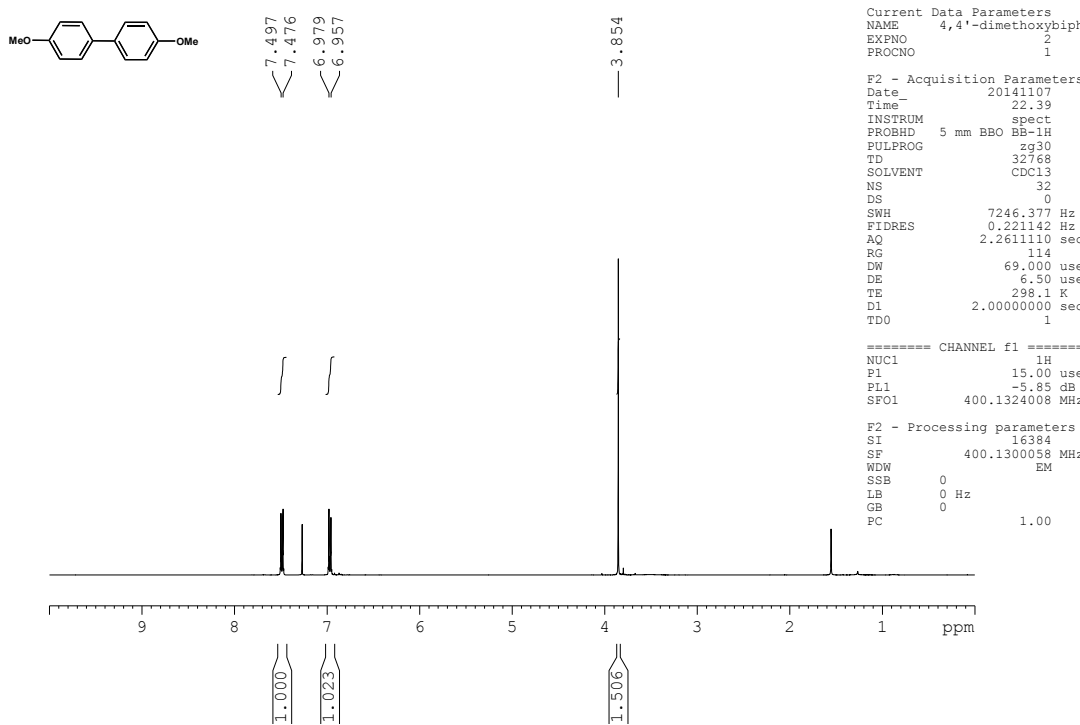
<sup>1</sup>H NMR (400 MHz, CDCl<sub>3</sub>, 25 °C)



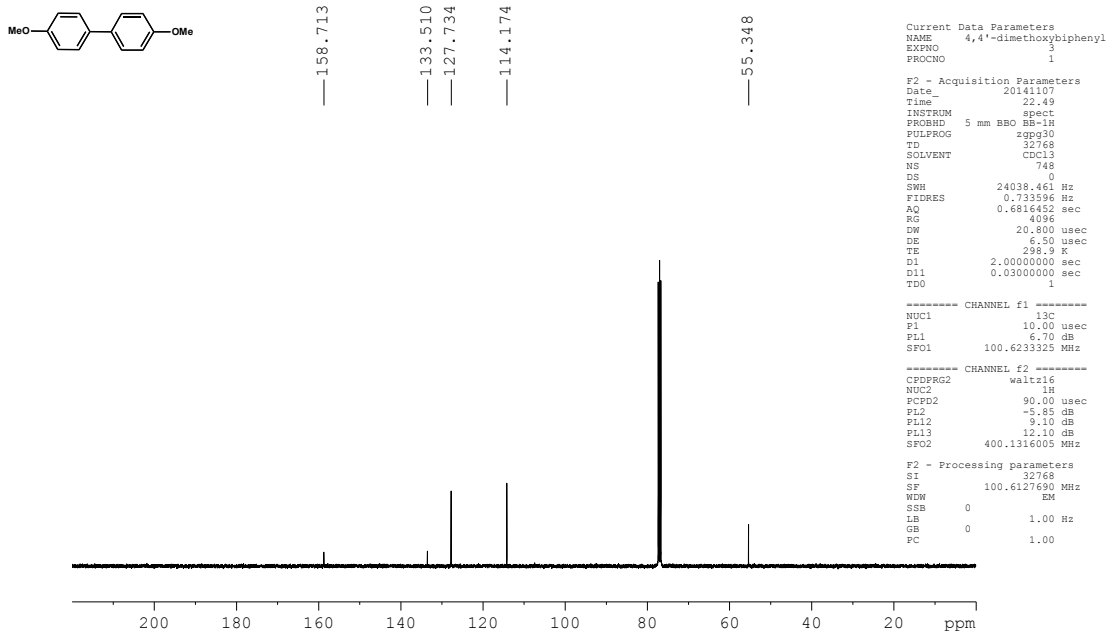
<sup>13</sup>C{<sup>1</sup>H} NMR (100 MHz, CDCl<sub>3</sub>, 25 °C)



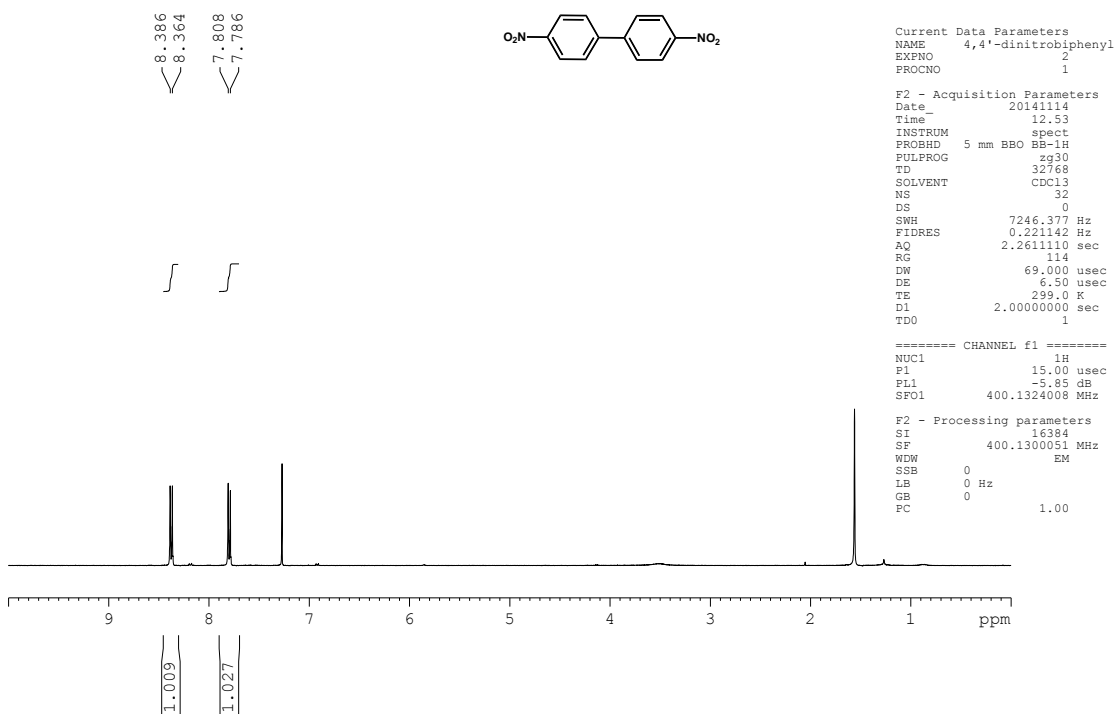
<sup>1</sup>H NMR (400 MHz, CDCl<sub>3</sub>, 25 °C)



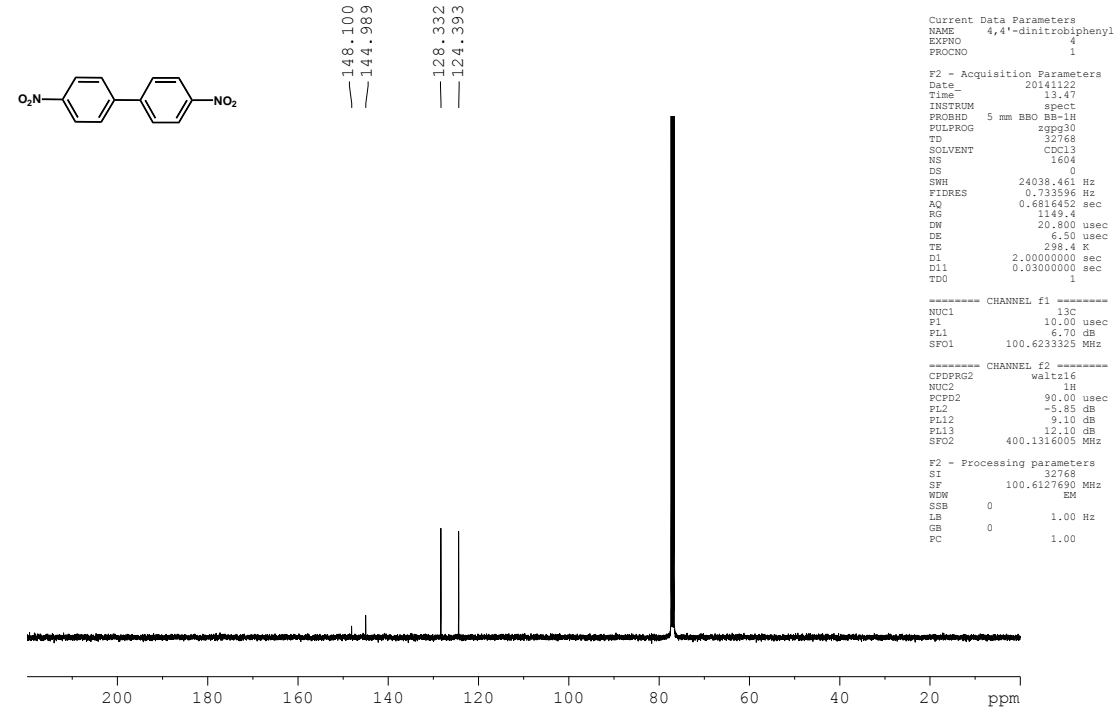
<sup>13</sup>C{<sup>1</sup>H} NMR (100 MHz, CDCl<sub>3</sub>, 25 °C)



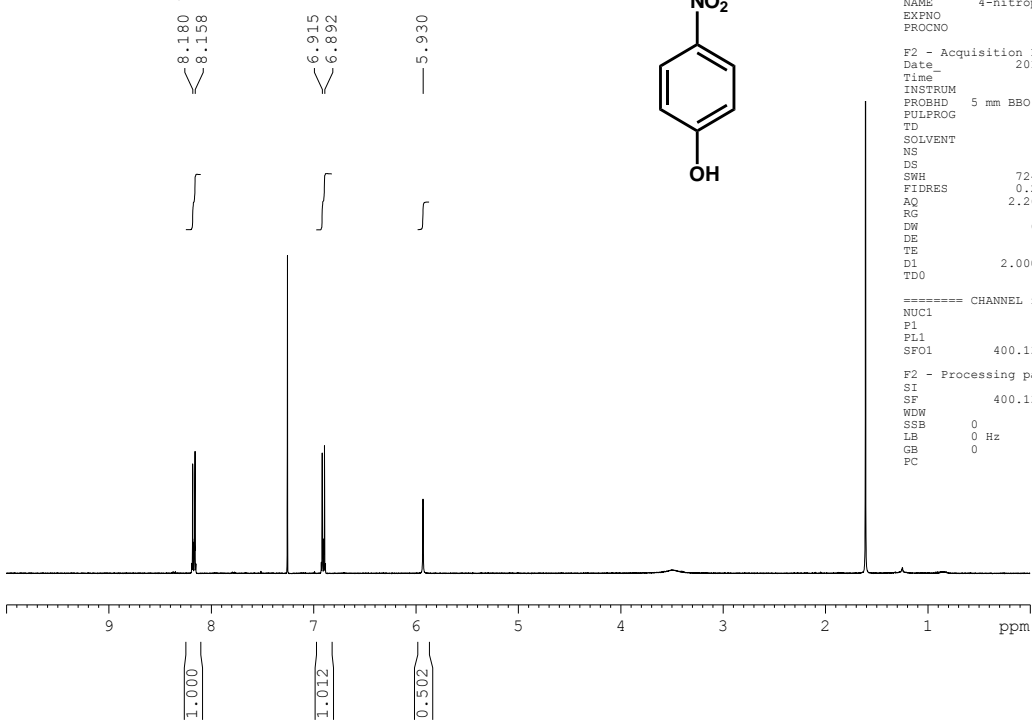
<sup>1</sup>H NMR (400 MHz, CDCl<sub>3</sub>, 25 °C)



<sup>13</sup>C{<sup>1</sup>H} NMR (100 MHz, CDCl<sub>3</sub>, 25 °C)



<sup>1</sup>H NMR (400 MHz, CDCl<sub>3</sub>, 25 °C)



<sup>13</sup>C{<sup>1</sup>H} NMR (100 MHz, CDCl<sub>3</sub>, 25 °C)

